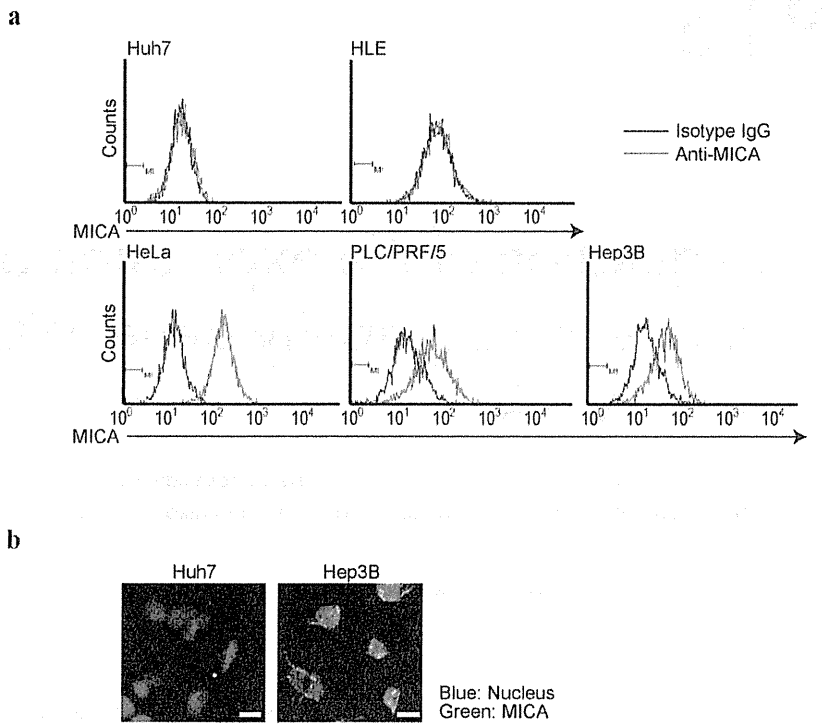

Figure 1 | Expression of MICA protein in HCC cells. (a), Flow cytometry assessment of MICA protein expression in HCC cells (purple lines). Isotype IgG was used for background staining (black lines). HeLa cells were used as the positive control. Representative results from two independent experiments are shown. (b), Immunofluorescence staining for MICA in Huh7 and Hep3B cells. Representative images from two independent experiments are shown. Scale bar, 25 μm.

Results

HCC cell lines differentially express MICA protein. To determine MICA protein levels in HCC cells, four representative HCC cell lines (Huh7, HLE, PLC/PRF/5, and Hep3B cells) underwent flow cytometry to evaluate MICA protein expression because no appropriate antibodies against MICA protein are at present available for western blotting. HeLa cells, which are known to express MICA protein[17], were used as a positive control. Hep3B and PLC/PRF/5 cells expressed substantial MICA protein levels, Huh7 and HLE cells expressed no MICA protein (Figure 1a). This was confirmed by immunocytochemistry using Huh7 and Hep3B cells, which showed staining mainly of cell surfaces (Figure 1b). These results suggest that the MICA protein expression status depends on the cell line examined, even those from the same organ.

The MiR25-93-106b cluster regulates MICA expression. Because upregulation of MICA expression was observed in Dicer-knockdown cells[18], we hypothesized that MICA expression levels may be at least partly regulated by miRNAs. We initially tested miRNAs that might affect MICA expression using reporter constructs into which MICA 3′-untranslated region (3′UTR) sequences were cloned and by transiently overexpressing 76 mature synthetic microRNAs, which were selected on the basis of their hepatic expression level, as in our previous studies[19,20]. Among the microRNAs examined, several may target MICA 3′UTR (Supplementary Figure 1). Among them, we focused on miR93 and miR106b, which were considered to target MICA 3′UTR based partly on the results of our initial miRNA testing described above; in addition, their possible target sequences were identified in the MICA 3′UTR sequences by a computational search using TargetScan 6.0 [21]. Additional reasons that we focused on these two miRNAs were as follows: 1) these miRNAs share the same seed sequences, to which two perfect-match complementary sequences exist in the 3′UTR of MICA (Figure 2a); 2) the target sequences are highly conserved among mammals and are thus likely to be biologically important sites; and 3) these miRNAs are located as a "miR25-93-106b cluster" on human chromosome 7q22.1, and so they may be expressed together under the same transcriptional control. We introduced mutations in the first possible miRNA target sequences of MICA 3′UTR in the reporter constructs (Supplementary Figure 2a); these sequences have a higher likelihood to be target sites, as determined by TargetScan. Co-transfection experiments revealed that reporter activity was suppressed by overexpression of a miR25-93-106b cluster-expressing plasmid (Figure 2b and Supplementary Figure 2b). The overexpression of an unrelated miR (let-7g)-expressing plasmid did not have any significant effects on the reporter activity (Supplementary Figure 2c) and the suppressive effect was lost using constructs with three point mutations in the seed sequences (Figure 2c), suggesting that miR25-93-106b directly targets these sequences and suppresses gene expression.

To confirm these effects, we generated HeLa and Hep3B cell lines that stably expressed the miR25-93-106b-cluster by transducing cells with miR25-93-106b-cluster-expressing lentiviruses (Figure 2d). As expected, the expression of the miR25-93-106b-cluster significantly suppressed MICA protein expression (Figure 2e). However, the expression levels of endogenous miR93 and 106b were not always proportional to the levels of MICA protein expression in the cell lines examined (Supplementary Figure 3). These results suggest that MICA protein expression can be regulated by miR93 and 106b, but that its expression is simultaneously endogenously regulated by other factors (possibly by promoter activities, including epigenetic changes).

Inhibition of miR25-93-106b function increases MICA protein expression. To develop methods of enhancing MICA protein expression levels based on the above results, we examined the

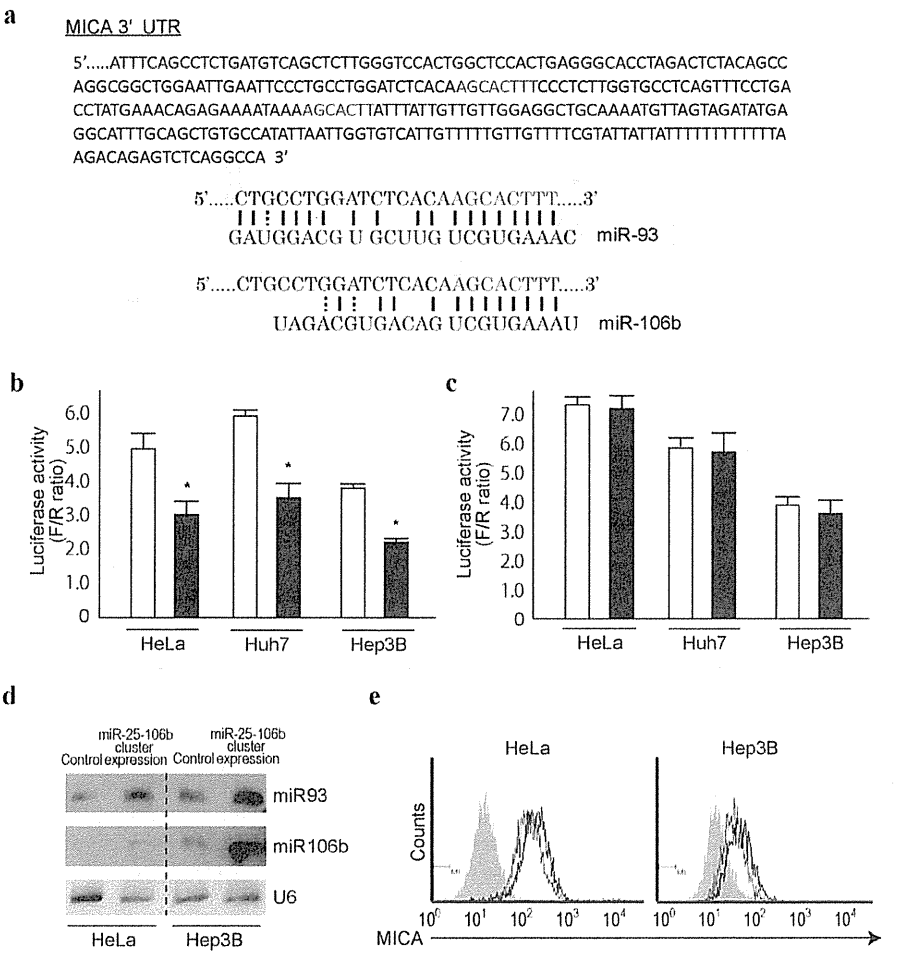

Figure 2 | miR93 and 106b target MICA 3′UTR. (a), Sequences of MICA 3′UTR (upper). Letters in red are the sequences completely matched with the seed regions of miR93 and 106b. The complementarities between the first predicted target in the MICA 3′UTR and miRNA sequences are shown below. (b), (c), Cells were co-transfected with pGL4-TK (renilla luciferase as an internal control), Luc-MICA-3′UTRwt (b) or Luc-MICA-3′UTRmut (c), and either an empty control vector (white bar) or miR25-93-106b-cluster expression plasmid (black bar). Data shows the means ± s.d. of the raw ratios (F/R) obtained by dividing firefly luciferase values with renilla luciferase values of three independent experiments. $^*p < 0.05$. (d), miR93 and miR106b expression levels in control and stably miR25-93-106b cluster-expressing cells were determined by northern blotting. U6 levels were used as a loading control. Representative images from two independent experiments are shown. Full-length blot images are available in Supplementary Figure 5. (e), Suppression of MICA expression by overexpression of miRNA93 and 106b. Flow cytometry assessment of MICA protein expression in control (black lines) and stably miR25-93-106b cluster-expressing HeLa and Hep3B cells (red lines). Gray-shaded histograms represent the background staining using isotype IgG. Representative results from two independent experiments are shown.

effects of functional downregulation of miR25-93-106b on MICA expression. We first performed a reporter assay of transient functional silencing of miR25-93-106b using a construct that produces mature anti-sense RNAs designed to silence miR25-93-106b function. As expected, the reporter activities with MICA 3′UTR sequences were enhanced by the functional silencing of miR25-93-106b in HeLa, Hep3B, and Huh7 cells (Figure 3a). However, such effects were not observed using mutant reporter constructs not targeted by those miRNAs (Figure 3b), suggesting that the enhancing effects of the reporter activities were miRNA-dependent.

Next, HeLa, Hep3B, and Huh7 cells were stably transduced with a lentivirus that expresses anti-sense RNAs as described above, and MICA protein expression levels were determined by flow cytometry. Consistent with the reporter assay results, MICA protein expression was increased in HeLa and Hep3B cells by the functional silencing of miR25-93-106b (Figure 3c). However, in Huh7 cells, which express no MICA protein in the normal state, silencing of miR25-93-106b had no effect on MICA protein expression (Figure 3c). These results suggest that MICA protein expression levels can be regulated by modulating miRNA function, albeit only if at least a small quantity of MICA protein is present. In contrast, modulation of miRNA function does not influence MICA protein expression levels when the MICA protein is not expressed, but this could be because there are other forms of regulation at extremely low levels.

MICA protein levels are related to tumor susceptibility to NK cells. To determine the consequences of the modulation of MICA protein expression levels by miRNAs, we first determined the binding ability of NKG2D, a receptor of MICA, using HeLa and Hep3B cells overexpressing the miR25-93-106b cluster or with silencing of miR25-93-106b function. As expected, the levels of NKG2D binding to the cells, theoretically through binding to MICA, were decreased in HeLa and Hep3B cells overexpressing the miR25-93-106b cluster (Figure 4a). On the contrary, the levels of NKG2D binding to the cells were increased in HeLa and Hep3B cells in which miR25-93-106b function had been silenced (Figure 4b).

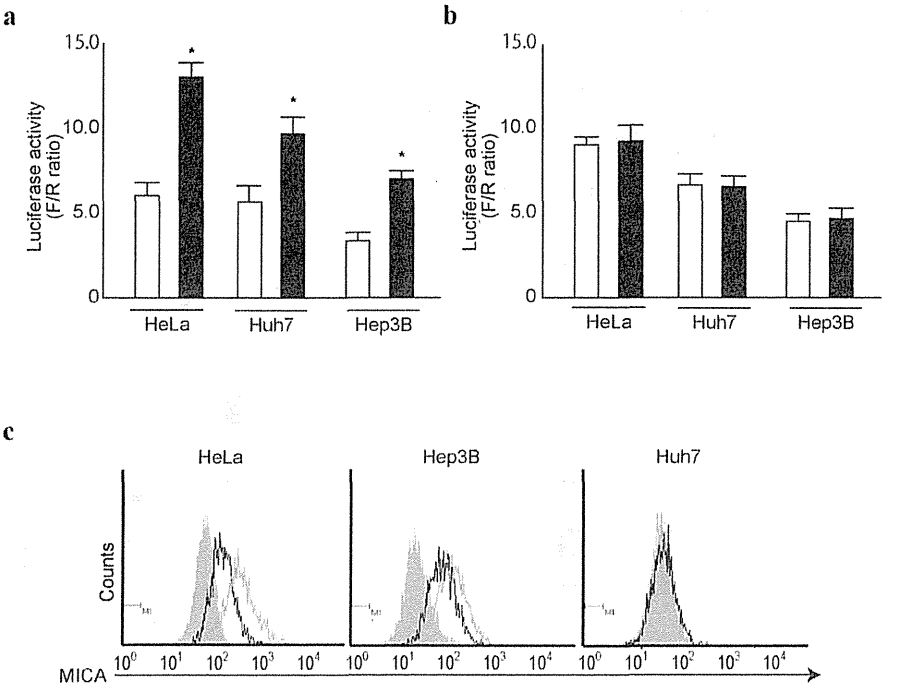

Figure 3 | Silencing of miR25-93-106b cluster enhances MICA expression. (a), (b), Cells were co-transfected with pGL4-TK (internal control), Luc-MICA-3′UTRwt (a) or Luc-MICA-3′UTRmut (b), and either an empty control vector (white bar) or plasmid expressing mature anti-sense sequences of miR25-93-106b cluster (black bar). Data shows the means ± s.d. of the raw ratios (F/R) obtained by dividing firefly luciferase values with renilla luciferase values of three independent experiments. $*p < 0.05$. (c), Enhancement of MICA expression by expression of anti-sense sequences of the miR25-93-106b cluster. Flow cytometry assessment of MICA protein expression in control (black lines) and stably mature anti-sense sequences of miR25-93-106b cluster-expressing cells (green lines). Gray-shaded histograms represent the background staining using isotype IgG. Representative results from three independent experiments are shown.

Next, to determine whether tumor cells with different miRNA-induced MICA protein expression levels exhibited differing susceptibilities to NK-cell-mediated killing *in vivo*, we performed a tumor-clearance assay that measures short-term *in vivo* killing by NK cells[22]. Hep3B control cells, Hep3B cells with miR25-93-106b cluster overexpression, or Hep3B cells with miR25-93-106b and HA-tagged MICA overexpression, labeled with fluorescent DiO, were injected into C57Black6/J mouse tail veins together with an equal number of HeLa cells labeled with Dil (internal reference control). After 5 h, surviving Hep3B and HeLa cells in the lungs were enumerated by flow cytometry. The number of Hep3B cells that had survived divided by the number of HeLa cells that had survived represents the relative killing of Hep3B cells *in vivo*. As shown by the *in vitro* binding assay using NKG2D, the killing rate of Hep3B cells in which miRNA function had been silenced was higher, and that of cells overexpressing miRNAs was lower, than that of control cells. The effects of miRNA overexpression were similar to those obtained in MICA knocked-down Hep3B cells (supplementary Figure 4). Additionally, the lower cell-killing rate in Hep3B cells overexpressing miRNA was antagonized by the co-expression of exogenous MICA protein (Figure 4c), suggesting that the decreased clearance was mediated by reduced MICA expression levels secondary to overexpression of miRNAs. These results suggest that tumor progression and invasion can be regulated by expression or silencing of miRNAs in at least some cells by regulation of MICA expression levels.

Discussion

In this study, we showed that the miR25-93-106b cluster modulates MICA protein expression by HCC cells. Because our previous GWAS analyses identified that MICA is the critical gene determining HCC susceptibility in patients with chronic hepatitis infection[5,6], the herein-described methods of modulating MICA expression may be useful for developing novel methods of prevention and therapeutics against HCCs.

MICA is a membrane protein that acts as a ligand for NKG2D to activate innate anti-tumor effects through natural killer and $CD8^+$ cells[7]. Our previous GWAS study showed that a risk allele at the SNP in the MICA promoter region was significantly associated with the susceptibility of HCV-induced HCC as well as with lower serum MICA levels. Although polymorphisms at the same SNP site were also associated with HBV-induced HCC, the risk allele determining the susceptibility of HCC was somehow different from that in HCV-induced HCC. While the reason why different MICA gene variations act as risk alleles at the same SNP site between HBV- and HCV-induced HCC has not been elucidated, it is assumed that changes in the membrane-bound MICA and soluble MICA levels due to differences in post-translational processing according to virus type may affect the risk allele results. In any case, because the importance of the regulation of MICA expression levels to prevent development of HCC due to chronic hepatitis viral infection cannot be denied, the regulation of MICA levels by microRNAs as shown here may be useful for the development of preventive methods of preventing HCC development during chronic hepatitis infection.

While several cellular signaling pathways lead to upregulation of MICA[12,13], we used microRNAs to regulate the expression levels of MICA in this study. As shown by the results of our GWAS analyses, which found that the polymorphisms in the promoter region of MICA are associated with changes in the sMICA levels[5,6], promoter activities of the MICA gene also have significant effects on MICA expression levels[23]. Our results showed that miR93 and 106b expression levels were not always correlated with those of MICA in HCC cell lines, suggesting that the regulation of MICA expression is not solely

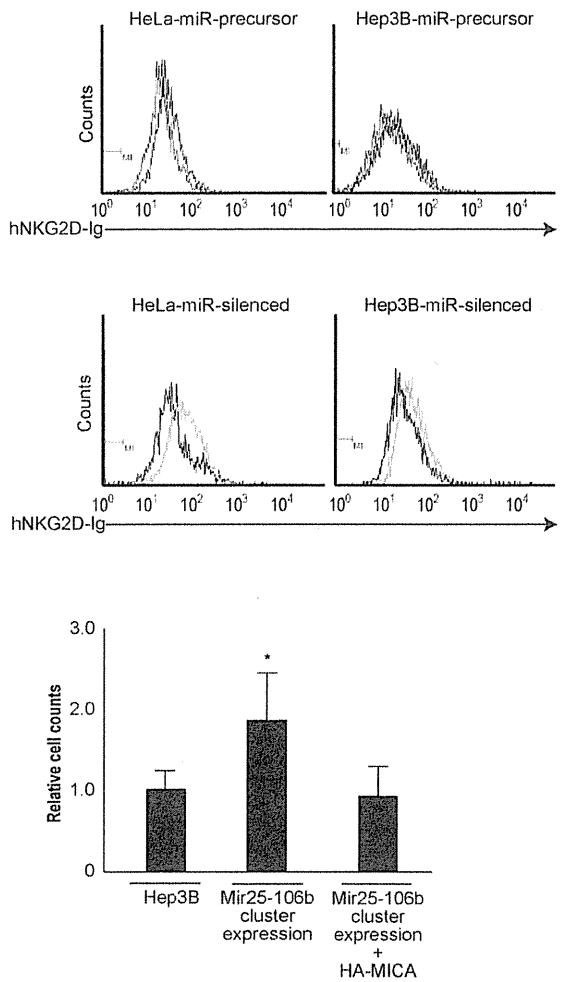

Figure 4 | NKG2D binding levels change in proportion to MICA expression levels. (a), (b), Flow cytometry of human IgG-fused NKG2D binding to the control (black lines), miR25-93-106b cluster-expressing cells (red lines) (a), and mature anti-sense sequences of miR25-93-106b cluster-expressing cells (green lines) (b). Representative results from three independent experiments are shown. (c), *In vivo* killing of DiO-labeled Hep3B and Dil-labeled HeLa cells (internal control cells) injected together into the tail veins of six mice in each group. Fluorescence intensities were quantified by flow cytometry as the ratio of Hep3B to HeLa cells in the lungs. The data from control Hep3B cells were set as 1.0. Data represent the means ± s.d. of three independent experiments. $^{*}p < 0.05$.

dependent on miRNAs. In addition, in cells with no endogenous MICA expression, such as Huh7 cells, modulation of microRNA expression had no effect on the regulation of MICA expression. This suggests that at least low-level endogenous expression, which may be determined by promoter activities, are needed for regulation by miRNA. Therefore, changes in promoter activities and epigenetic changes in the MICA gene should also be determined. This will facilitate application of the regulatory function of miRNAs reported here.

One class of antisense oligonucleotides, namely locked nucleic acids, can be used to sequester microRNAs in the liver of various animals, including humans[16,24,25]. A clinical trial targeting miR-122 with the anti-miR-122 oligonucleotides miravirsen, the first miRNA-targeted drug, is underway for the treatment of HCV infection[16]. Thus, nucleic-acid-mediated gene therapy is becoming a realistic option. Modulation of MICA expression levels by such nucleic-acid-mediated therapy based on the results presented herein may also be a promising option for prevention and/or therapy of HCC.

In summary, we have shown that the miR25-93-106b cluster can be used to modulate MICA expression levels in HCC cells. Based on our GWAS results and associated studies, regulation of MICA protein expression levels is crucial to prevent the development of HCC during chronic hepatitis viral infection. It is important to identify the other factors that regulate MICA transcriptional activities as well as the post-translational processes and their association with susceptibility to HCCs. That said, miRNA regulation of MICA expression as shown here may facilitate regulation of the host innate immune system in an HCC-suppressive manner during chronic hepatitis viral infection.

Methods

Cell culture. The human HCC cell lines Huh7, HLE, PLC/PRF/5, and Hep3B were obtained from the Japanese Collection of Research Bioresources (JCRB, Osaka, Japan). The human cervical cancer cell line HeLa was obtained from the American Type Culture Collection (ATCC, Rockville, MD). All cells were maintained in Dulbecco's modified Eagle's medium supplemented with 10% fetal bovine serum.

Mouse. Experimental protocols were approved by the Ethics Committee for Animal Experimentation at the Graduate School of Medicine, the University of Tokyo and the Institute for Adult Disease, Asahi Life Foundation, Japan and conducted in accordance with the Guidelines for the Care and Use of Laboratory Animals of the Department of Medicine, the University of Tokyo, and the Institute for Adult Disease, Asahi Life Foundation.

Flow cytometry. Cells were hybridized with anti-MICA (1 : 500; R&D Systems, Minneapolis, MN) and isotype control IgG (1 : 500; R&D Systems) in 5% BSA/1% sodium azide/PBS for 1 h at 4°C. After washing, cells were incubated with goat anti-mouse Alexa 488 (1 : 1000; Molecular Probes, Eugene, OR) for 30 min. Flow cytometry was performed and data analyzed using Guava Easy Cyte Plus (GE Healthcare, Little Chalfont, UK).

Reporter plasmid construction, transient transfections, and luciferase assays. The reporter plasmid for the analysis of the effects of miRNAs on MICA 3′UTR were constructed by subcloning the MICA 3′UTR sequences from pLightSwitch-MICA 3UTR (SwitchGear Genomics, Menlo Park, CA) into the pGL4.50 vector (Promega, Madison, WI) at the *FseI* site by the In-Fusion method (Clontech, Mountain View, CA) to insert the MICA 3′UTR sequences into the 3′-UTR of the firefly luciferase gene, which was under the control of the CMV promoter. The sequences of the primers were 5′-CTA GAG TCG GGG CGG CG GCC ATT TCA GCC TCT GAT GTC AGC-3′ and 5′-GTC TGC TCG AAG CGG CCG GCC TGG CCT GAG ACT CTG TCT TAA-3′. The resultant plasmid (Luc-MICA 3′UTRwt) was used as a template for the construction of mutant reporter plasmid (Luc-MICA 3′UTRmut), which carries three point mutations in the seed sequences of miR93 and 106b in the MICA 3′UTR, itself generated by a Quik Change II XL Site-directed Mutagenesis Kit (Stratagene, Heidelberg, Germany) according to the manufacturer's instructions. Transient transfection and reporter assays were performed as described previously[26].

Lentiviral constructs, viral production, and transduction. To generate a neomycin-resistant miR25-93-106b cluster-expressing lentiviral construct, copGFP in the pmiRNA25-93-106b cluster-expressing plasmid (System Biosciences, Mountain View, CA) was replaced with a neomycin resistant gene, which was subcloned from the pCDH-Neo vector (System Biosciences), at the *FseI* site. The primers used were 5′-GCT ACC GCT ACG AGG CCG GCC CAT GAT TGA ACA AGA TGG ATT GCA-3′ and 5′-TCG CCG ATC ACG CGG CCG GCC TCA GAA GAA CTC GTC AAG AAG GC-3′. To remove the copGFP region from pmiRZIP25-93-106b (System Biosciences), a construct expressing mature anti-sense sequences of the miR25-93-106b cluster, sequences coding the GFP gene were removed by excision with *XbaI* and *PstI* sites followed by connecting the cut ends with annealed oligonucleotides (5′-CTA GAC GCC ACC ATG CTG CA-3′ and 5′-GCA TGG TGG CGT-3′) to maintain the coding frame and the expression of the downstream puromycin-resistance gene. To generate HA-tagged MICA protein overexpressing the lentiviral construct, MICA cDNA was amplified by PCR using a Halo-tag-MICA–expressing plasmid (Promega, Madison, WI) as a template and cloned into a pCDH-puro vector (System Biosciences) at the *NotI* site. The primer sequences used were 5′-ATC GGA TCC GCG GCC GCA CCA TGT ACC CAT ACG ATG TTC CAG ATT ACG CTA TGG GGC TGG GCC CGG TC-3′ and 5′-AGA TCC TTC GCG GCC GCT TAG GCG CCC TCA GTG GAG C-3′. Let-7g precursor expressing plasmid was generated by inserting about 1,000 bp long PCR product around the let-7g genomic region into pCDH-puro vector using *Xba*1 and *Not*1 sites. The production and concentration of lentiviral particles were described previously[27]. shRNA against MICA-producing lentiviral particles with puromycin resistant gene were purchased from SantaCruz Biotechnology (sc-4924-V, Dallas, TX). Cells were transduced with lentiviruses using

polybrene (EMD Millipore, Billerica, MA). The selections were performed with 400 μg/mL G418 and 2 μg/mL (HeLa) or 6 μg/mL (Hep3B) puromycin.

Immunocytochemistry. Cells on two-well chamber slides were fixed with 4% paraformaldehyde. Fixed cells were probed with the primary MICA antibody (R&D Systems) for 1 h after blocking with 5% normal goat serum for 30 min. Cells probed with the MICA antibody were incubated with the secondary Alexa Fluor 488 goat anti-mouse antibody (Molecular Probes) for 30 min. Slides were mounted using VectaShield with DAPI (Vector Labs, Burlingame, CA).

Northern blotting of miRNAs. Northern blotting of miRNAs was performed as described previously[27]. Briefly, total RNA was extracted using TRIzol Reagent (Invitrogen, Carlsbad, CA) according to the manufacturer's instructions. Ten micrograms of RNA were resolved in denaturing 15% polyacrylamide gels containing 7 M urea in 1 × TBE and then transferred to a Hybond N+ membrane (GE Healthcare) in 0.25 × TBE. Membranes were UV-crosslinked and prehybridized in hybridization buffer. Hybridization was performed overnight at 42°C in ULTRAhyb-Oligo Buffer (Ambion) containing a biotinylated probe specific for miR93 (cta cct gca cga aca gca ctt tg) and 106b (atc tgc act gtc agc act tta), which had previously been heated to 95°C for 2 min. Membranes were washed at 42°C in 2 × SSC containing 0.1% SDS, and the bound probe was visualized using a BrightStar BioDetect Kit (Ambion). Blots were stripped by boiling in a solution containing 0.1% SDS and 5 mM EDTA for 10 min prior to rehybridization with a U6 probe (cac gaa ttt gcg tgt cat cct t).

miRNA library screening. To screen for miRNAs that target MICA 3′-UTR, synthetic miRNA mimics and reporter constructs were used as described previously[19,20]. Seventy-six types of synthetic mature miRNAs that are highly expressed in the liver[28] were custom-made (B-Bridge, Tokyo, Japan) and transfected by RNAi Max (Life Technologies, Carlsbad, CA) into Huh7 cells in 96-well plates that had been transfected 24 h before with Luc-MICA 3′UTRwt. The cells were then incubated for another 24 h. As negative controls, oligonucleotides of artificial sequences were applied[19]. The luciferase activities were measured using a GloMax 96 Microplate Luminometer (Promega). The experiments were performed in duplicate.

NKG2D binding assay. Cells were incubated with 4 μg of recombinant human NKG2D fused to human IgG1 Fc chimera protein. After washing, cells were incubated with an Alexa488-conjugated affinity purified F(ab')2 fragment of goat anti-human IgG (Jackson ImmunoResearch Laboratories, West Grove, PA). As a negative control, cells were incubated with only Alexa488 anti-human IgG. The intensity of the fluorescence was determined by flow cytometry.

***In vivo* cell-killing assay.** Hep3B cells and HeLa cells were labeled with the fluorescent dye VybrantDiO and DiI (Molecular Probes), respectively. Cells were mixed at a density of 2×10^7 in 1-ml PBS, and 200 μl was injected into the tail vein. Five hours later, lungs were collected, and single-cell suspensions were collected using a cell strainer. Fluorescence was assayed by flow cytometry, and the ratio of the experimental Hep3B cells to HeLa cells (internal control) was calculated.

Statistical analysis. Statistically significant differences between groups were determined using Student's *t*-test when variances were equal. When variances were unequal, Welch's *t*-test was used instead. *P*-values of < 0.05 were considered to indicate statistical significance.

1. El-Serag, H. B. Epidemiology of viral hepatitis and hepatocellular carcinoma. *Gastroenterology* **142**, 1264–1273 (2012).
2. Sherman, M. Hepatocellular carcinoma: New and emerging risks. *Dig Liver Dis* **42**, S215–222 (2010).
3. Arzumanyan, A., Reis, H. M. & Feitelson, M. A. Pathogenic mechanisms in HBV- and HCV-associated hepatocellular carcinoma. *Nat Rev Cancer* **13**, 123–135 (2013).
4. Urabe, Y. *et al.* A genome-wide association study of HCV-induced liver cirrhosis in the Japanese population identifies novel susceptibility loci at the MHC region. *J Hepatol* (2013).
5. Kumar, V. *et al.* Genome-wide association study identifies a susceptibility locus for HCV-induced hepatocellular carcinoma. *Nat Genet* **43**, 455–458 (2011).
6. Kumar, V. *et al.* Soluble MICA and a MICA variation as possible prognostic biomarkers for HBV-induced hepatocellular carcinoma. *PLoS One* **7**, e44743 (2012).
7. Maccalli, C., Scaramuzza, S. & Parmiani, G. TNK cells (NKG2D+ CD8+ or CD4+ T lymphocytes) in the control of human tumors. *Cancer Immunol Immunother* **58**, 801–808 (2009).
8. Jinushi, M. *et al.* Impairment of natural killer cell and dendritic cell functions by the soluble form of MHC class I-related chain A in advanced human hepatocellular carcinomas. *J Hepatol* **43**, 1013–1020 (2005).
9. Diefenbach, A., Jensen, E. R., Jamieson, A. M. & Raulet, D. H. Rae1 and H60 ligands of the NKG2D receptor stimulate tumour immunity. *Nature* **413**, 165–171 (2001).
10. Hayakawa, Y. Targeting NKG2D in tumor surveillance. *Expert Opin Ther Targets* **16**, 587–599 (2012).
11. Guerra, N. *et al.* NKG2D-deficient mice are defective in tumor surveillance in models of spontaneous malignancy. *Immunity* **28**, 571–580 (2008).
12. Bauer, S. *et al.* Activation of NK cells and T cells by NKG2D, a receptor for stress-inducible MICA. *Science* **285**, 727–729 (1999).
13. Eleme, K. *et al.* Cell surface organization of stress-inducible proteins ULBP and MICA that stimulate human NK cells and T cells via NKG2D. *J Exp Med* **199**, 1005–1010 (2004).
14. Yadav, D., Ngolab, J., Lim, R. S., Krishnamurthy, S. & Bui, J. D. Cutting edge: down-regulation of MHC class I-related chain A on tumor cells by IFN-gamma-induced microRNA. *J Immunol* **182**, 39–43 (2009).
15. Stern-Ginossar, N. & Mandelboim, O. An integrated view of the regulation of NKG2D ligands. *Immunology* **128**, 1–6 (2009).
16. Janssen, H. L. *et al.* Treatment of HCV Infection by Targeting MicroRNA. *N Engl J Med* **368**, 1685–94 (2013).
17. Salih, H. R., Rammensee, H. G. & Steinle, A. Cutting edge: down-regulation of MICA on human tumors by proteolytic shedding. *J Immunol* **169**, 4098–4102 (2002).
18. Tang, K. F. *et al.* Decreased Dicer expression elicits DNA damage and up-regulation of MICA and MICB. *J Cell Biol* **182**, 233–239 (2008).
19. Takata, A. *et al.* MicroRNA-22 and microRNA-140 suppress NF-κB activity by regulating the expression of NF-κB coactivators. *Biochem Biophys Res Commun* **411**, 826–831 (2011).
20. Yoshikawa, T. *et al.* Silencing of microRNA-122 enhances interferon-a signaling in the liver through regulating SOCS3 promoter methylation. *Sci. Rep.* **2**, 637 (2012).
21. Lewis, B. P., Burge, C. B. & Bartel, D. P. Conserved seed pairing, often flanked by adenosines, indicates that thousands of human genes are microRNA targets. *Cell* **120**, 15–20 (2005).
22. Gazit, R. *et al.* Lethal influenza infection in the absence of the natural killer cell receptor gene Ncr1. *Nat Immunol* **7**, 517–523 (2006).
23. Lo, P. H. *et al.* Identification of a Functional Variant in the MICA Promoter Which Regulates MICA Expression and Increases HCV-Related Hepatocellular Carcinoma Risk. *PLoS One* **8**, e61279 (2013).
24. Lanford, R. E. *et al.* Therapeutic silencing of microRNA-122 in primates with chronic hepatitis C virus infection. *Science* **327**, 198–201 (2010).
25. Elmén, J. *et al.* LNA-mediated microRNA silencing in non-human primates. *Nature* **452**, 896–899 (2008).
26. Kojima, K. *et al.* MicroRNA122 is a key regulator of α-fetoprotein expression and influences the aggressiveness of hepatocellular carcinoma. *Nat Commun* **2**, 338 (2011).
27. Takata, A. *et al.* MicroRNA-140 acts as a liver tumor suppressor by controlling NF-κB activity by directly targeting DNA methyltransferase 1 (Dnmt1) expression. *Hepatology* **57**, 162–170 (2013).
28. Krützfeldt, J. *et al.* Silencing of microRNAs in vivo with 'antagomirs'. *Nature* **438**, 685–689 (2005).

Acknowledgments

This work was supported by Grants-in-Aid from the Ministry of Education, Culture, Sports, Science and Technology, Japan (#25293076, #25460979, and #24390183) (to M.Otsuka, Y.K. and K.K.), by Health Sciences Research Grants of The Ministry of Health, Labour and Welfare of Japan (to K.K.), and by grants from the Okinaka Memorial Institute for Medical Research, the Liver Forum in Kyoto, and the Princess Takamatsu Cancer Research Fund (to M.Otsuka).

Author contributions

T.K., M. Otsuka and K.K. planned the research and wrote the paper. T.K., M. Otsuka, T.Y., M. Ohno, A.T., C.S. and Y.K. performed the majority of the experiments. M.A. and H.Y. supported several experiments and analyzed the data. K.K. supervised the entire project.

Additional information

Supplementary information accompanies this paper at http://www.nature.com/scientificreports

Competing financial interests: The authors declare no competing financial interests.

How to cite this article: Kishikawa, T. *et al.* Regulation of the expression of the liver cancer susceptibility gene MICA by microRNAs. *Sci. Rep.* 3, 2739; DOI:10.1038/srep02739 (2013).

Biochemical and Biophysical Research Communications 432 (2013) 22–27

Contents lists available at SciVerse ScienceDirect

Biochemical and Biophysical Research Communications

journal homepage: www.elsevier.com/locate/ybbrc

Overexpression of gankyrin in mouse hepatocytes induces hemangioma by suppressing factor inhibiting hypoxia-inducible factor-1 (FIH-1) and activating hypoxia-inducible factor-1

Yu Liu [a], Hiroaki Higashitsuji [a,*], Hisako Higashitsuji [a], Katsuhiko Itoh [a], Toshiharu Sakurai [b], Kazuhiko Koike [c], Kiichi Hirota [d], Manabu Fukumoto [e], Jun Fujita [a,*]

[a] Department of Clinical Molecular Biology, Graduate School of Medicine, Kyoto University, 54 Shogoin Kawaharacho, Sakyo-ku, Kyoto 606-8507, Japan
[b] Department of Gastroenterology and Hepatology, Faculty of Medicine, Kinki University, 377-2 Ohno-Higashi, Osaka-Sayama, Osaka 589-8511, Japan
[c] Department of Gastroenterology, Graduate School of Medicine, The University of Tokyo, 7-3-1 Hongo, Bunkyo-ku, Tokyo 113-8655, Japan
[d] Department of Anesthesia, Kyoto University Hospital, 54 Shogoin-Kawaracho, Sakyo-Ku, Kyoto 606-8507, Japan
[e] Department of Pathology, Institute of Development, Aging and Cancer, Tohoku University, Sendai 980-8575, Japan

ARTICLE INFO

Article history:
Received 22 January 2013
Available online 1 February 2013

Keywords:
PSMD10
HIF-1
FIH-1
Oncogene
Hemangioma

ABSTRACT

Gankyrin (also called p28 or PSMD10) is an oncoprotein commonly overexpressed in hepatocellular carcinomas. It consists of 7 ankyrin repeats and interacts with multiple proteins including Rb, Cdk4, MDM2 and NF-κB. To assess the oncogenic activity *in vivo*, we produced transgenic mice that overexpress gankyrin specifically in the hepatocytes. Unexpectedly, 5 of 7 F2 transgenic mice overexpressing hepatitis B virus X protein (HBX) promoter-driven gankyrin, and one of 3 founder mice overexpressing serum amyloid P component (SAP) promoter-driven gankyrin developed hepatic vascular neoplasms (hemangioma/hemangiosarcomas) whereas none of the wild-type mice did. Endothelial overgrowth was more frequent in the livers of diethylnitrosamine-treated transgenic mice than wild-type mice. Mouse hepatoma Hepa1-6 cells overexpressing gankyrin formed tumors with more vascularity than parental Hepa1-6 cells in the transplanted mouse skin. We found that gankyrin binds to and sequester factor inhibiting hypoxia-inducible factor-1 (FIH-1), which results in decreased interaction between FIH-1 and hypoxia-inducible factor-1α (HIF-1α) and increased activity of HIF-1 to promote VEGF production. The effects of gankyrin were more prominent under 3% O_2 than 1% or 20% O_2 conditions. Thus, the present study clarified, at least partly, mechanisms of vascular tumorigenesis, and suggests that gankyrin might play a physiological role in hypoxic responses besides its roles as an oncoprotein.

1. Introduction

Gankyrin (also called p28, $p28^{GANK}$ or PSMD10) was identified as an oncoprotein commonly overexpressed in hepatocellular carcinomas (HCCs) [1]. Gankyrin was also independently isolated as p28, a supposed component of the 26S proteasome, but recent studies have demonstrated that p28 associates only with free 19S particles of the 26S proteasome or their precursors and functions as a chaperone to guide their assembly [2]. As expected for a protein consisting of 7 ankyrin repeats [3], gankyrin interacts with multiple proteins and shows a variety of activities. For example, gankyrin binds to Rb and Cdk4, and accelerates phosphorylation and degradation of Rb to activate DNA synthesis genes [1]. Gankyrin binds to the E3 ubiquitin ligase MDM2, thereby facilitating ubiquitylation and degradation of p53 [4]. Gankirin binds to NF-κB and suppresses its activity by modulating acetylation via SIRT1 [5]. Gankyrin binds to hepatocyte nuclear factor 4α, which determines hepatocyte differentiation status and enhances its degradation [6]. Gankyrin activates PI3K/AKT/mTOR/hypoxia-inducible factor-1 (HIF-1) signaling [7].

Most solid tumors contain hypoxic regions, and one of the most important cellular factors involved in the hypoxic response which promotes angiogenesis, anaerobic metabolism and resistance to apoptosis is HIF-1 [8,9]. HIF-1 is a heterodimeric transcription factor composed of a constitutively expressed β subunit and an inducibly expressed α subunit (HIF-1α). Under aerobic conditions, HIF-1α is hydroxylated by specific prolyl hydroxylases at two conserved Pro residues in a reaction requiring oxygen. Hydroxylation

Abbreviations: CAD, C-terminal transactivation domain; DEN, diethylnitrosamine; FIH-1, factor inhibiting hypoxia-inducible factor-1; firefly-luciferase, F-Luc; H&E, hematoxylin and eosin; HBX, hepatitis B virus X protein; HCC, hepatocellular carcinoma; HIF, hypoxia-inducible factor; RT-qPCR, reverse transcription-quantitative polymerase chain reaction; SAP, serum amyloid P component.

* Corresponding authors. Fax: +81 75 7514977.
E-mail addresses: hhigashi@virus.kyoto-u.ac.jp (H. Higashitsuji), jfujita@virus.kyoto-u.ac.jp (J. Fujita).

0006-291X/$ - see front matter © 2013 Elsevier Inc. All rights reserved.
http://dx.doi.org/10.1016/j.bbrc.2013.01.093

facilitates binding of von Hippel–Lindau protein, a component of the ubiquitin protein ligase, to HIF-1α, leading to its proteasomal degradation. The ability of HIF-1α to activate transcription is also prevented by factor inhibiting HIF-1 (FIH-1) [8–10]. FIH-1 hydroxylates a specific Asn residue in HIF-1α, and disrupts interaction of HIF-1α with the transcription co-activators p300 and CBP. Under hypoxic conditions, prolyl hydroxylase and FIH-1 activities are inhibited by substrate (O_2) deprivation, resulting in HIF-1α stabilization and binding to the p300/CBP complex, thus allowing HIF transactivation.

Since gankyrin plays important roles in cell proliferation and apoptosis, is overexpressed in most HCCs, and confers tumorigenicity to non-malignant cells, we produced transgenic mice that overexpressed gankyrin specifically in the hepatocytes to assess its oncogenic activity *in vivo*. Unexpectedly, the mice developed vascular tumors (hemangioma/hemangiosarcomas) in the liver, and so we have tried to elucidate the underlying mechanisms for vascularization.

2. Materials and methods

2.1. Transgenic mice

To express gankyrin specifically in the liver, cDNA for the mouse wild-type gankyrin N-terminally tagged with 2× FLAG was cloned into the pBEPBglII expression vector containing the hepatitis B virus X protein (HBX) promoter [11]. Fertilized eggs were obtained from C57BL/6J mice, and transgenic mice were produced at the Center for Animal Resources and Development, Kumamoto University, Japan. A plasmid containing the human serum amyloid P component (SAP) promoter [12] and expressing mouse wild-type gankyrin N-terminally tagged with 3× FLAG was also constructed, and transgenic mice were produced with this at the Genome Information Research Center, Osaka University, Japan, using eggs from D2B6F1 mice. For genotyping, DNA was extracted from the tail of each mouse and analyzed by Southern blotting using gankyrin cDNA as probe.

2.2. Treatment of mice

A single intraperitoneal injection of diethylnitrosamine (DEN, Sigma, 25 mg/kg of body weight) was administered to 14-days-old transgenic and control male mice. Groups of animals were euthanized at 8 months after injection, and the livers were removed, examined for visible lesions, and paraffin embedded after fixation in 10% buffered formalin.

For tumor formation, cells (2×10^6) were suspended in 0.1 ml of PBS and injected subcutaneously into the back of athymic BALB/c mice (Japan SLC Inc.). Each mouse received Hepa1-6 cells on one side and Hepa1-6/GK cells on the other side. All experiments involving mice were approved by the Animal Research Committee of Kyoto University, and conducted in accordance with the institutional and NIH guidelines for the care and use of laboratory animals.

2.3. Human materials

Eighteen specimens of HCC were taken by needle biopsy before initiation of the treatment at Kinki University Hospital, Japan. The study protocol was approved by the institutional review boards, and written informed consent was obtained from all patients for subsequent use of their collected tissues.

2.4. Cell culture and DNA transfection

U-2 OS cells, HEK293 cells, HEK293T cells, mouse hepatoma Hepa1-6 cells and their transfectants were maintained in Dulbecco's modified Eagle's medium supplemented with 10% fetal bovine serum at 37 °C and 5% CO_2 as described [4]. For mild hypoxic conditions, cells were placed in a modular incubator chamber and flushed with a gas mixture containing 1 or 3% O_2, 5% CO_2, and balance N2.

Calcium phosphate-DNA coprecipitation method was used for DNA transfection. Plasmids encoding, gankyrin, shRNA for gankyrin, HIF-1α, FIH-1, and their fusion proteins have been described previously [4,5,10,13].

2.5. Pathologicall analyses

The immunohistochemical staining was performed on 4-μm-thick paraffin sections of tissues fixed in 10% buffered formalin as described [14]. The sections were incubated with the primary antibodies against endothelial cell markers CD31 (dianoba GmbH) and CD34 (Abnova), followed by horseradish peroxidase-conjugated anti-rat immunoglobulin antibody (Santa Cruz Biotechnology), and were developed in Diaminobenzidine colorimetric reagent solution (DAKO). They were counterstained with hematoxylin. To assess the presence of the atypical proliferative lesion of endothelial cells, at least 1 section from 4 lobes were examined under a microscope.

2.6. Analyses of gene expression and protein interactions

Preparation of cell lysates, immunoprecipitation, and Western blot analysis were performed as described [4]. Rabbit polyclonal anti-gankyrin, anti-VEGF-A, anti-HIF-1α, anti-FIH-1, anti-β-actin, and biotin-conjugated anti-HA antibodies (all from Santa Cruz Biotech.), anti-Myc tag antibody (MBL), anti-FLAG and biotin-conjugated anti-FLAG antibodies (Sigma), mouse monoclonal anti-HA antibody (Roche), and rabbit polyclonal antibody raised against recombinant mouse gankyrin were used as the primary antibodies in Western blotting.

For immunoprecipitation, mouse anti-HA antibody (Roche), rabbit anti-FLAG antibody, and biotin-conjugated anti-FLAG and anti-HA antibodies were used.

Reverse transcription-quantitative polymerase chain reaction (RT-qPCR) analysis was done as described [14]. The relative levels of gankyrin and VEGF-A mRNAs were determined by RT-qPCR using β-actin and GAPDH mRNA for normalization. Primer sequences used were as follows: gankyrin (human, 5′-TCTTCAAGCCATCCTGTGTG-3′ and 5′-TGGTGATGTTGGACTCCTCA-3′), VEGF-A (human, 5′-AAAA CTGCT GGTGTCCCAAG-3′ and 5′-ATTAAACCCAGGCCACCTTT-3′; mouse, 5′-CA GGCTGCTGTAACGATGAA-3′ and 5′-TATGTGCTGGCTTTGGTGAG-3′), β-actin (human, CTACGTCGCCCTGGACTTCGAGC and GATGGAGC CGCCGATCCACACGG), GAPDH (mouse, 5′-ACAACTTTGTC AAGCT-CATTTCCTG-3′ and 5′-TGGTCCAGGGTTTCTTACTCCTTGG-3′).

2.7. Reporter assays

The reporter plasmids p2.1 and p2.4 contain wild-type and mutant copies, respectively, of the hypoxia response element (HRE) from the *ENO1* gene upstream of an SV40 promoter and firefly luciferase (F-Luc) coding sequences [13]. U-2 OS cells were cotransfected with either p2.1 or p2.4, pRL vector expressing Renilla luciferase (pRL-CMV, Promega) and plasmids expressing HA-FIH-1 and FLAG-gankyrin or gankyrin-shRNA [4].

The GAL4 reporter plasmid GAL4E1bLuc containing five GAL4-binding sites upstream of an E1b TATA sequence and the F-Luc gene, and GAL4-expressing plasmids GalA(531–826) and

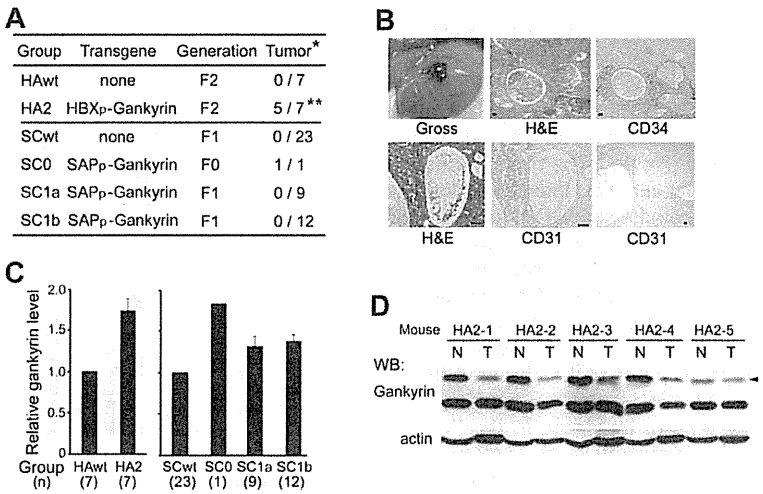

Fig. 1. Vascular tumors in gankyrin-transgenic mice. (A) Incidence of hepatic tumors. Gankyrin was expressed in hepatocytes by using HBX promoter (HBXp) or SAP promoter (SAPp). *number of mice with hepatic tumors at 22 months of age/total number of mice. **$P < 0.05$ compared with HAwt group. (B) Gross and microscopic appearances of hepatic vascular lesions in transgenic mice. H&E, hematoxylin and eosin staining. CD31 and CD34, immunoperoxidase staining for CD31 and CD34, respectively, using diaminobenzidine as substrate. Bar, 50 μm. (C) Gankyrin expression in the non-tumorous liver. Lysates prepared from indicated mice were analyzed by Western blotting and densitometry. Bars are average ± SD of total gankyrin levels normalized with actin levels, and expressed as relative to those of wild-type mice. (D) Expression of endogenous and exogenous (arrowhead) gankyrin in the tumor (T) and non-tumorous portion (N) of the liver from indicated F2 transgenic mice. Western blot analysis.

GalA-N803 expressing the C-terminal transactivation domain (CAD) of the wild-type and FIH-1-insensitive HIF-1α, respectively, fused to the GAL4 DNA-binding domain were described previously [15]. U-2 OS cells were cotransfected with GAL4E1bLuc, pRL-CMV, GAL4-expressing plasmids, and plasmids expressing FLAG-gankyrin or gankyrin-shRNA.

Transfected cells were exposed to mild hypoxia (1 or 3% O_2) for 48 h and harvested for dual luciferase assays (Promega) as described [5].

2.8. Statistical analysis

To determine whether the means of two groups are significantly different from each other, the Student's *t*-test and chi-square test were used. All statistical analyses including Fisher's exact probability test were performed using the JMP software (SAS Institute). A *P* value less than 0.05 was considered statistically significant.

3. Results

3.1. Vascular neoplasms developed in the liver of gankyrin-transgenic mouse

The HBX promoter [11] was first used to direct hepatocyte-specific expression of the wild-type gankyrin in transgenic mice. Two founder (F0) mice were obtained and subsequently mated with wild-type mice to produce F1 offspring containing the transgene. F1 mice were then mated with wild-type mice to produce F2 offspring. When F0, F1 and F2 mice were sacrificed at 9–13 months

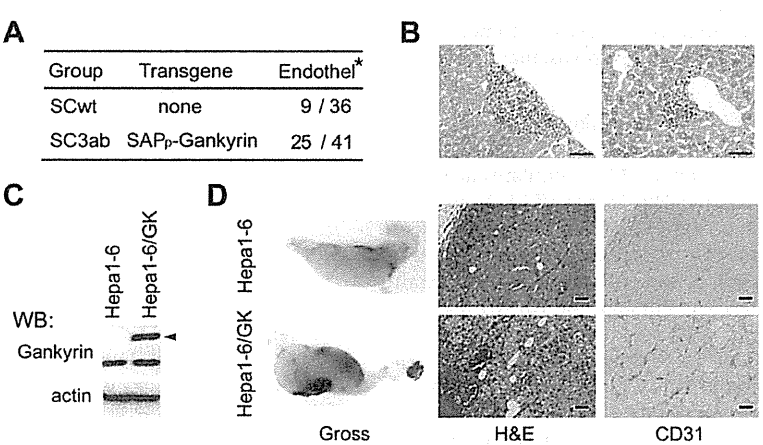

Fig. 2. Increased vascularity of hepatic tumors overexpressing gankyrin. (A) Vascularity in the livers of gankyrin-transgenic (SC3ab) and wild-type (SCwt) mice with diethylnitrosamine (DEN)-induced HCCs. Eight months after DEN treatment, mice were sacrificed and tumor vascularity was evaluated microscopically. *Number of mice with endothelial overgrowth in the liver/number of mice administered DEN. $P < 0.05$ between these groups. (B) Typical examples of atypical proliferation of endothelial cells in (A). H&E stain. Bar, 50 μm. (C) Expression of endogenous and exogenous (arrowhead) gankyrin in Hepa1-6 and Hepa1-6/GK cells analyzed by Western blotting. (D) Vascularity of Hepa1-6 and Hepa1-6/GK tumors in nude mouse skin. Typical gross and microscopic (H&E and immunoperoxidase staining of CD31) appearances of formalin-fixed paraffin-embedded tumors. Bar, 50 μm.

of age, no hepatic tumor was observed (data not shown). At 22 months of age, however, 5 of the remaining 7 male F2 developed hepatic vascular tumors, whereas no tumor was found in the control mice (Fig. 1A and B). The protein level of gankyrin in the non-tumorous liver of transgenic mice was about 1.7-fold compared with that of wild-type mice (Fig. 1C). The tumors consisted of large somewhat irregular vascular channels lined by endothelial cells. In some areas elongated or spindle-shaped endothelial cells lined vascular spaces, formed solid sheets, with an atypical nucleus, suggesting malignancy (Fig. 1B). Immunohisochemical analysis demonstrated that the tumor cells expressed the endothelial cell markers CD31 and CD34. The expression of gankyrin was less in the vascular tumors than non-tumorous liver tissues (Fig. 1D). Taken together, these results indicated that the observed tumors were hemangioma/hemangiosarcomas.

To increase the expression level of transgene in the liver, we next produced gankyrin-transgenic mice using the SAP promoter [12]. At the age of 22 months, one of the 3 F0 mice developed hemangioma/hemangiosarcomas, but none of its F1 offspring and other 2 F0 mice (Fig. 1A). In the F0 with vascular tumors, the transgene was integrated into more than one locus, resulting in inheritance of less integration sites and lower levels of gankyrin expression in the offspring (Fig. 1C and data not shown).

3.2. Increased vascularity in tumors overexpressing gankyrin

To evaluate the effect of gankyrin on angiogenesis in the liver, we used the DEN-induced hepatocarcinogenesis model. At 8 months after DEN treatment, 100% of wild-type mice and SAP promoter-driven gankyrin-transgenic mice (F4) developed hepatocarcinomas. Multiplicity of tumors was not different between the two groups, but the incidence of microscopic vascular lesions characterized by angiectasis and atypically proliferating endothelial cells was significantly higher in the transgenic mice than wild-type mice (Fig. 2A and B).

To further examine the effect of gankyrin on neovasculization, we stably overexpressed FLAG-tagged gankyrin in mouse Hepa1-6 hepatoma cells (Hepa1-6/GK cells, Fig. 2C). Two weeks after inoculation, both Hepa1-6 and Hepa1-6/GK cells formed tumors, and tumor vascularity was grossly more prominent in the Hepa1-6/GK tumors compared with Hepa1-6 tumors in all 6 mice inoculated (Fig. 2D). Immunohistochemical staining with anti-CD31 endothelial marker antibody demonstrated increased blood vessel density in Hepa1-6/GK tumors compared with Hepa1-6 tumors. Thus, overexpression of gankyrin increased the neovascularization.

3.3. Increased VEGF expression induced by gankyrin

Since HIF-1-mediated expression of VEGF stimulates angiogenesis [8,9], we analyzed expression of HIF-1α and VEGF-A. As shown in Fig. 3A, expression levels of VEGF-A protein and mRNA were higher in the livers of gankyrin-transgenic mice compared to wild-type mice. Overexpression of gankyrin in Hepa1-6 cells also increased protein level of VEGF-A, although the HIF-1α level was not increased. (Fig. 3B).

Transcriptional activation of the VEGF gene in response to hypoxia is mediated by binding of HIF-1 to HRE [13]. To examine whether gankyrin affects transcriptional activity mediated by HRE, we transfected U-2 OS cells with HRE-Luc reporter plasmid. Gankyrin enhanced the luciferase activity induced by mild hypoxia (3% O_2) by 4-fold, but only 1.5-fold or no enhancement at 1% or 20% O_2 concentration, respectively (Fig. 3C and data not shown). Conversely, suppression of gankyrin expression by shRNA reduced the luciferase activity. When HRE was mutated, the luciferase activity was not increased by hypoxia, and the enhancing effect

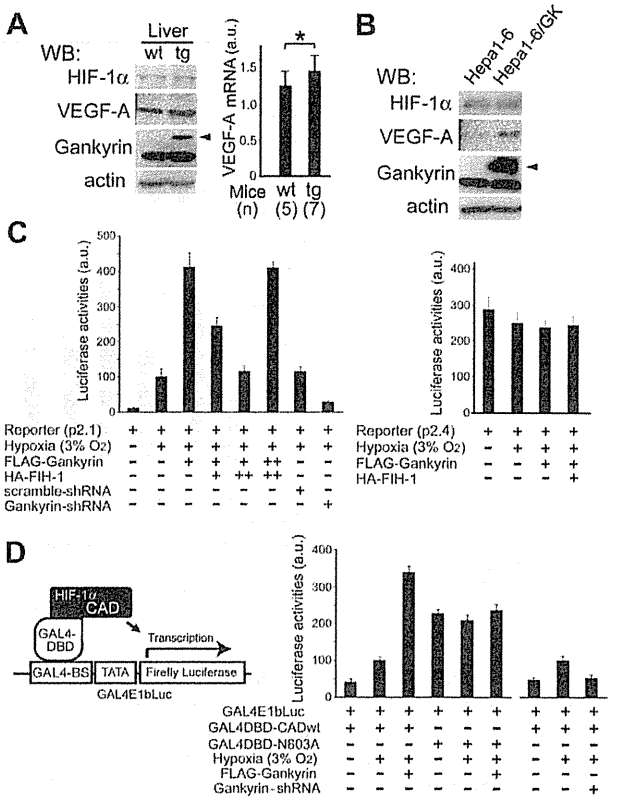

Fig. 3. Increased VEGF expression induced by gankyrin. (A) VEGF-A and HIF-1α expression in the livers of wild-type (wt) and gankyrin-transgenic (tg) mice. Western blotting (left) and RT-qPCR (right). Arrowhead, FLAG-Gankyrin. VEGF-A transcript levels were normalized with GAPDH levels. Values are average ± SD. $^*P < 0.05$. a.u., arbitrary unit. (B) Effects of gankyrin on expression of VEGF-A. Hepa1-6 cells and Hepa1-6 transfectants overexpressing FLAG-Gankyrin (Hepa1-6/GK) were analyzed by Western blotting. Arrowhead, FLAG-Gankyrin. (C) HRE-dependent transcriptional activation. U-2 OS cells were cotransfected with *ENO1*–F-luciferase (Luc) reporter plasmids (p2.1) or mutated reporter plasmids lacking the HIF-1 recognition sequence (p2.4), and plasmids expressing R-Luc, FLAG-Gankyrin, HA–FIH-1, gankyrin-shRNA, and scrambled-shRNA as indicated. 48 h later, some dishes were transferred to hypoxic conditions. After further 48-h incubation, cell lysates were analyzed for Luc activity. F-Luc activity was normalized with R-Luc activity. Values are average ± SD from 3 independent experiments. a.u., arbitrary unit. (D) Asn803-dependent increase in HIF-1α transcriptional activity. U-2 OS cells were cotransfected with Gal4–F-Luc reporter plasmids (GAL4E1bLuc), plasmids expressing GAL4 DNA-binding domain (DBD) fused to wild-type (wt) or N803A mutant C-terminal half (CAD) of HIF-1α, R-Luc, and FLAG-Gankyrin and gankyrin-shRNA as indicated. After 48 h of hypoxic incubation, Luc activities were measured and expressed as in (C). GAL4-BS, GAL4-binding sites. a.u., arbitrary unit.

of gankyrin was not observed, indicating that the effect was mediated by HRE.

We next examined whether gankyrin affects transcriptional activity of HIF-1α. We employed a reporter system composed of the F-Luc gene whose expression is controlled by GAL4-binding elements (GAL4E1bLuc, Fig. 3D) and the HIF1α-CAD fused to the GAL4 DNA-binding domain [13]. Compared with normoxia (20% O_2), luciferase activity was 2.5-fold higher at 3% O_2 concentration (Fig. 3D). Overexpression of gankyrin further increased the HIF-1α activity by 3-fold, whereas suppression of gankyrin reduced it. At 1% or 20% O_2 concentration, however, these effects of gankyrin were not observed (data not shown). When fusion protein of HIF-1α-CAD mutated at Asn803 was used, gankyrin showed no effect. Since Asn803 is the critical residue for FIH-1 to inhibit HIF-1α activity, these results suggest that the effect of gankyrin was mediated by FIH-1.

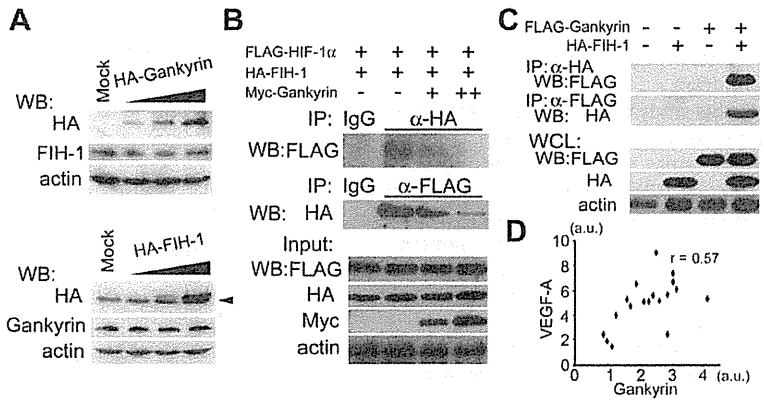

Fig. 4. Binding of gankyrin to FIH-1. (A) Effect of gankyrin on FIH-1 protein level. HEK293 cells were transfected with increasing amounts of plasmids expressing HA-gankyrin or HA-FIH-1, or empty vector (Mock) as indicated. 48 h later, cell lysates were analyzed by Western blotting. Arrowhead, non-specific bands. (B) Effect of gankyrin on binding of HIF-1α to FIH-1. HEK293T cells were cotransfected with plasmids expressing FLAG–HIF-1α, HA–FIH-1, and Myc-tag-gankyrin, and cultured at 3% O_2 for 48 h. Cell lysates were immunoprecipitated (IP), and precipitants and inputs were analyzed by Western blotting (WB) using the indicated antibodies. (C) Interaction of gankyrin with FIH-1. HEK293T cells were cotransfected with plasmids expressing FLAG-Gankyrin and HA-FIH-1, and cultured at 3% O_2 for 48 h. Cell lysates were immunoprecipitated, and precipitants and inputs were analyzed by WB as in (B). WCL, whole cell lysates. Experiments were repeated three times with similar results. (D) Scatter plot of mRNA levels of gankyrin and VEGF-A in human hepatocellular carcinoma specimens. a.u., arbitrary unit.

3.4. Sequestration and inhibition of FIH-1 by gankyrin

We examined whether or not gankyrin suppresses FIH-1 expression. Overexpression of gankyrin did not affect FIH-1 level (Fig. 4A). When FIH-1 was overexpressed, the gankyrin level did not change, either. Thus, we suspected that gankyrin might affect the interaction of FIH-1 and HIF-1α. As shown in Fig. 4B, binding of FIH-1 and HIF-1α was suppressed by gankyrin. As FIH-1 binds ankyrin repeat domain proteins [16] and gankyrin contains 7 ankyrin repeats [3], we checked the possibility that gankyrin binds to FIH-1. HA-FIH-1 and FLAG-gankyrin were coimmunoprecipitated by either anti-HA or anti-FLAG antibody from cells cultured at 3% O_2, but not or only slightly at 1% or 20% O_2 concentration, respectively (Fig. 4C and data not shown). These results demonstrate that gankyrin binds to and sequester FIH-1, resulting in decreased interaction between FIH-1 and HIF-1α and increased activity of HIF-1 under mild hypoxic conditions. When we further examined the mRNA levels of gankyrin and VEGF-A in biopsy specimens of human HCC, a moderate positive correlation ($r = 0.57$, $P < 0.02$) was found (Fig. 4D), suggesting that the gankyrin–FIH-1 interaction might have some clinical relevance.

4. Discussion

Hemangioma/hemangiosarcomas are occasionally seen in mouse liver with incidences less than 3% [17]. In the present study, 71% of the F2 transgenic mice overexpressing HBX promoter-driven gankyrin developed hepatic hemangioma/hemangiosarcomas, whereas none of the wild-type mice did. This phenotype was probably not due to random insertional mutagenesis in the transgenic mice as it was also observed in F0 mice expressing SAP promoter-driven gankyrin. In the subsequent generations of this F0, however, gankyrin levels were decreased and no hemangioma/hemangiosarcoma developed. The finding that mice with 70% increase, but none with 35% increase in the protein level of hepatic gankyrin developed hemangioma/hemangiosarcomas (Fig. 1C) suggests that there is a critical level of gankyrin to show this phenotype.

How does overexpression of gankyrin in hepatocytes induce endothelial cell-derived tumors? As gankyrin induces dedifferentiation of HCCs [6], it may also induce transdifferentiation of hepatocytes into endothelial cells. A more feasible explanation, however, would be that gankyrin facilitates a sustained release of angiogenic growth factors, providing the milieu leading to hemangiosarcoma formation [18]. Consistent with this notion, endothelial overgrowth was more frequent in the HCCs of gankyrin-transgenic mice than wild-type mice after DEN treatment. Furthermore, mouse hepatoma transfectants overexpressing gankyrin induced more neovasculariation than parental cells when subcutaneously inoculated into nude mice. VEGF-A was the first identified member of the VEGF family, and mice with transgenic VEGF-A expressed in the liver have increased vascularization and vascular permeability [19]. When myoblasts overexpressing VEGF-A are transplanted into limb or heart muscle of mice, they induce hemangiomas [20]. In the present study, VEGF-A level was higher in the liver of gankyrin-transgenic mice compared with wild-type mice, and gankyrin increased VEGF-A expression in cultured hepatoma cells. Thus, VEGF-A probably contributed to formation of hemangioma/hemangiosarcomas in the gankyrin-transgenic mice.

HIF-1 is a major factor regulating the level of VEGF, and despite induction of multiple angiogenic target genes such as adrenomedullin and placental growth factor, VEGF is essential for HIF-1 mediated neovascularization [21]. Hypoxia induces changes in the hydroxylation status of well-conserved Pro and Asn residues of HIF-1α, resulting in protein stabilization and transcriptional activation [8,9]. Signaling through receptor tyrosine kinases induce HIF-1 expression by increasing the rate of HIF-1α protein synthesis via PI3K/Akt/mTOR pathway [8], and gankyrin activates this to promote VEGF expression [7]. In the present study, the HIF-1α protein level was not increased in cells overexpressing gankyrin. Reporter assays indicated, however, that HIF-1 transcriptional activity was increased by gankyrin, and that it was dependent on Asn803 of HIF-1α. FIH-1 hydroxylates this residue and inhibits transcriptional activity [8–10]. In addition to HIF-1α, proteins containing ankyrin repeat domains are common targets for hydroxylation by FIH-1, and IκBα as well as Notch-1 block the FIH-1-mediated HIF-1α repression by sequestering FIH-1 [22]. In this case, the recognition of each substrate and their relative affinity for FIH-1 is an important determinant of FIH-1 sequestration and consequently HIF regulation. Consistent with the recent study using recombinant proteins [16], gankyrin and FIH-1 were co-immunoprecipitated from cell lysates. Furthermore, overexpression of gankyrin reduced the amount of HIF-1α bound to FIH-1, suggesting a higher affinity for FIH-1 of gankyrin than HIF-1α at mild hypoxia. As expected, gankyrin increased the HIF-1 transcriptional activity in reporter

assays, which was dependent on FIH-1. Interestingly, the binding of gankyrin to FIH-1 and enhancement of HIF-1 activity were dependent on the O_2 concentration.

We have demonstrated in this study that sustained overexpression of gankyrin in hepatocytes, although at a low level, can induce liver hemangioma/hemangiosarcomas in mice. Gankyrin sequesters FIH-1 from HIF-1α to activate HIF-1 and increase production of VEGF, which at least partly contributes to hemangioma/hemangiosarcoma formation. Further studies will clarify why spontaneous hemangioma/hemangiosarcomas are extremely rare in humans in contrast to experimental animals [18], and shed light on mechanisms of vascular tumorigenesis as well as hepatocarcinogeneis. The present study also suggests that gankyrin might play a physiological role in hypoxic responses besides its roles as an oncoprotein.

Acknowledgments

We thank Profs. R.J. Mayer, University of Nottingham, U.K. and Ryuzo Sakata, Kyoto University for helpful suggestions, and Ms. Fumiyo Kataoka for technical assistance. This work was partly supported by Grants-in-Aid for Scientific Research from the Ministry of Education, Culture, Sports, Science and Technology of Japan, the Japan Society for the Promotion of Science, Cooperative Research Project Program of IDAC, Tohoku University, Global COE Program "Center for Frontier Medicine", MEXT, Japan, and the Japan Smoking Research Foundation.

References

[1] H. Higashitsuji, K. Itoh, T. Nagao, et al., Reduced stability of retinoblastoma protein by gankyrin, an oncogenic ankyrin-repeat protein overexpressed in hepatomas, Nat. Med. 6 (2000) 96–99.
[2] H.C. Besche, A. Peth, A.L. Goldberg, Getting to first base in proteasome assembly, Cell 138 (2009) 25–28.
[3] S. Krzywda, A.M. Brzozowski, H. Higashitsuji, et al., The crystal structure of gankyrin, an oncoprotein found in complexes with cyclin-dependent kinase 4, a 19 S proteasomal ATPase regulator, and the tumor suppressors Rb and p53, J. Biol. Chem. 279 (2004) 1541–1545.
[4] H. Higashitsuji, H. Higashitsuji, K. Itoh, et al., The oncoprotein gankyrin binds to MDM2/HDM2, enhancing ubiquitylation and degradation of p53, Cancer Cell 8 (2005) 75–87.
[5] H. Higashitsuji, H. Higashitsuji, Y. Liu, et al., The oncoprotein gankyrin interacts with RelA and suppresses NF-kappaB activity, Biochem. Biophys. Res. Commun. 363 (2007) 879–884.
[6] W. Sun, J. Ding, K. Wu, et al., Gankyrin-mediated dedifferentiation facilitates the tumorigenicity of rat hepatocytes and hepatoma cells, Hepatology 54 (2011) 1259–1272.
[7] J. Fu, Y. Chen, J. Cao, et al., P28GANK overexpression accelerates hepatocellular carcinoma invasiveness and metastasis via phosphoinositol 3-kinase/AKT/hypoxia-inducible factor-1α pathways, Hepatology 53 (2011) 181–192.
[8] G.L. Semenza, HIF-1: upstream and downstream of cancer metabolism, Curr. Opin. Genet. Dev. 20 (2010) 51–56.
[9] M.Y. Koh, G. Powis, Passing the baton: the HIF switch, Trends Biochem. Sci. 37 (2012) 364–372.
[10] P.C. Mahon, K. Hirota, G.L. Semenza, FIH-1: a novel protein that interacts with HIF-1alpha and VHL to mediate repression of HIF-1 transcriptional activity, Genes Dev. 15 (2001) 2586–2675.
[11] K. Koike, K. Moriya, K. Ishibashi, et al., Expression of hepatitis C virus envelope proteins in transgenic mice, J. Gen. Virol. 76 (1995) 3031–3038.
[12] K. Araki, O. Hino, J. Miyazaki, K. Yamamura, Development of two types of hepatocellular carcinoma in transgenic mice carrying the SV40 large T-antigen gene, Carcinogenesis 12 (1991) 2059–2062.
[13] G.L. Semenza, B.H. Jiang, S.W. Leung, Hypoxia response elements in the aldolase A, enolase 1, and lactate dehydrogenase A gene promoters contain essential binding sites for hypoxia-inducible factor 1, J. Biol. Chem. 271 (1996) 32529–32537.
[14] A. Umemura, Y. Itoh, K. Itoh, et al., Association of gankyrin protein expression with early clinical stages and insulin-like growth factor-binding protein 5 expression in human hepatocellular carcinoma, Hepatology 47 (2008) 493–502.
[15] B.H. Jiang, J.Z. Zheng, S.W. Leung, et al., Transactivation and inhibitory domains of hypoxia-inducible factor 1alpha, J. Biol. Chem. 272 (1997) 19253–19260.
[16] S.E. Wilkins, S. Karttunen, R.J. Hampton-Smith, et al., Factor inhibiting HIF (FIH) recognizes distinct molecular features within hypoxia-inducible factor-α (HIF-α) versus ankyrin repeat substrates, J. Biol. Chem. 287 (2012) 8769–8781.
[17] T. Harada, A. Enomoto, G.A. Boorman, R.R. Maronpot, Liver and gallbladder, in: R.R. Maronpot (Ed.), Pathology of the Mouse, Cache River Press, Vienna, IL, 1999, pp. 119–183.
[18] S.M. Cohen, R.D. Storer, K.A. Criswell, et al., Hemangiosarcoma in rodents: mode-of-action evaluation and human relevance, Toxicol. Sci. 111 (2009) 4–18.
[19] P. Leppänen, I. Kholová, A.J. Mähönen, et al., Short and long-term effects of hVEGF-A(165) in Cre-activated transgenic mice, PLoS One 1 (2006) e13.
[20] M.L. Springer, A. Banfi, J. Ye, et al., Localization of vascular response to VEGF is not dependent on heparin binding, FASEB J. 21 (2007) 2074–2085.
[21] S. Oladipupo, S. Hu, J. Kovalski, et al., VEGF is essential for hypoxia-inducible factor-mediated neovascularization but dispensable for endothelial sprouting, Proc. Natl. Acad. Sci. USA 108 (2011) 13264–13269.
[22] D.H. Shin, S.H. Li, S.W. Yang, et al., Inhibitor of nuclear factor-kappaB alpha derepresses hypoxia-inducible factor-1 during moderate hypoxia by sequestering factor inhibiting hypoxia-inducible factor from hypoxia-inducible factor 1alpha, FEBS J. 276 (2009) 3470–3480.

Journal of Clinical Virology 57 (2013) 173–177

Contents lists available at SciVerse ScienceDirect

Journal of Clinical Virology

journal homepage: www.elsevier.com/locate/jcv

Case report

Uninodular combined hepatocellular and cholangiocarcinoma with multiple non-neoplastic hypervascular lesions appearing in the liver of a patient with HIV and HCV coinfection

Koji Uchino[a], Ryosuke Tateishi[a,*], Hayato Nakagawa[a], Junichi Shindoh[b], Yasuhiko Sugawara[b], Masaaki Akahane[c], Junji Shibahara[d], Haruhiko Yoshida[a], Kazuhiko Koike[a]

[a] Department of Gastroenterology, Graduate School of Medicine, The University of Tokyo, Tokyo, Japan
[b] The Artificial Organ and Transplantation Division, Department of Surgery, Graduate School of Medicine, The University of Tokyo, Tokyo, Japan
[c] Department of Radiology, Graduate School of Medicine, The University of Tokyo, Tokyo, Japan
[d] Department of Pathology, Graduate School of Medicine, The University of Tokyo, Tokyo, Japan

ARTICLE INFO

Article history:
Received 27 August 2012
Received in revised form 2 December 2012
Accepted 18 January 2013

Keywords:
Combined hepatocellular and cholangiocarcinoma
Human immunodeficiency virus
Hepatitis C virus
Highly active antiretroviral therapy

ABSTRACT

A 42-year-old man suffering from haemophilia A and coinfection of human immunodeficiency virus (HIV) and hepatitis C virus was referred to our institution because of multiple liver tumours. He had been receiving highly active antiretroviral therapy for HIV infection. Ultrasonography showed multiple hypoechoic space-occupying lesions in the liver. Contrast-enhanced dynamic computed tomography (CT) and magnetic resonance imaging revealed multiple ring-enhanced hypervascular lesions in the liver. An ultrasonography-guided biopsy was performed and histological evaluation indicated one of the lesions to be combined hepatocellular and cholangiocarcinoma and others to be non-neoplastic. The patient underwent partial hepatic resection and is currently alive without recurrence for 15 months. Multiple ring-enhanced lesions have been undetectable in postoperative follow-up CT examinations.

1. Why this case is important

Because of shared routes of viral transmission, coinfection with human immunodeficiency virus (HIV) and hepatitis C virus (HCV) is not uncommon.[1,2] As a result of advances in highly active antiretroviral therapy (HAART), the morbidity and mortality associated with HIV infection have declined. Instead, HCV-related liver disease, including cirrhosis and hepatocellular carcinoma (HCC), and hepatotoxic effects associated with antiretroviral drugs have become major problems for patients coinfected with HIV and HCV.[3] We report a case of multiple hepatic hypervascular lesions appearing in a patient coinfected with HIV and HCV, which were found to be solitary combined hepatocellular and cholangiocarcinoma (cHCC-CC) accompanied by non-neoplastic lesions.

2. Case report

A 42-year-old man suffering from haemophilia A and coinfection of HIV and HCV was referred to our institution because of liver tumours. He had been examined periodically with ultrasonography but no liver tumours had been detected until then. The patient had been treated with atazanavir, ritonavir and tenofovir disoproxil/emtricitabine for HIV infection and remained asymptomatic. He did not take any medicine including herbal medicines other than the antiviral drugs described above. Blood-test results at the referral were: albumin, 3.7 g dl^{-1}; total bilirubin, 3.1 mg dl^{-1}; direct bilirubin, 1.1 mg dl^{-1}; aspartate aminotransferase, 65 IU l^{-1}; alanine aminotransferase, 44 IU l^{-1}; alkaline phosphatase, 623 IU l^{-1}; gamma-glutamyl transpeptidase, 149 IU l^{-1}; platelet count, 122×10^3 μl^{-1}; international normalised ratio of prothrombin time, 0.93; alpha-foetoprotein (AFP), 73 ng ml^{-1}; lens culinaris agglutinin-reactive fraction of AFP, 5.6%; des-gamma-carboxy prothrombin, 28 mAU ml^{-1}; carcinoembryonic antigen, 3.0 ng ml^{-1}; carbohydrate antigen 19-9, 119 U ml^{-1}; and CD4 count 177 cells μl^{-1}. HIV1-RNA was not detectable and HCV-RNA was 7.2 Log IU ml^{-1}. Blood culture was negative. Ultrasonography showed multiple hypoechoic lesions in the liver with a maximum diameter of 1.8 cm (Fig. 1A–C). One nodule in the segment 5 was more sharply marginated than other

Abbreviations: AFP, alpha-foetoprotein; cHCC-CC, combined hepatocellular and cholangiocarcinoma; CT, computed tomography; Gd-EOB-DTPA, gadolinium-ethoxybenzyl-diethylenetriamine pentaacetic acid; HAART, highly active antiretroviral therapy; HCC, hepatocellular carcinoma; HCV, hepatitis C virus; HIV, human immunodeficiency virus; MRI, magnetic resonance imaging.

* Corresponding author at: Department of Gastroenterology, Graduate School of Medicine, The University of Tokyo, 7-3-1 Hongo, Bunkyo-ku, Tokyo 113-8655, Japan. Tel.: +81 3 3815 5411; fax: +81 3 3814 0021.
E-mail address: tateishi-tky@umin.ac.jp (R. Tateishi).

1386-6532/$ – see front matter © 2013 Elsevier B.V. All rights reserved.
http://dx.doi.org/10.1016/j.jcv.2013.01.012

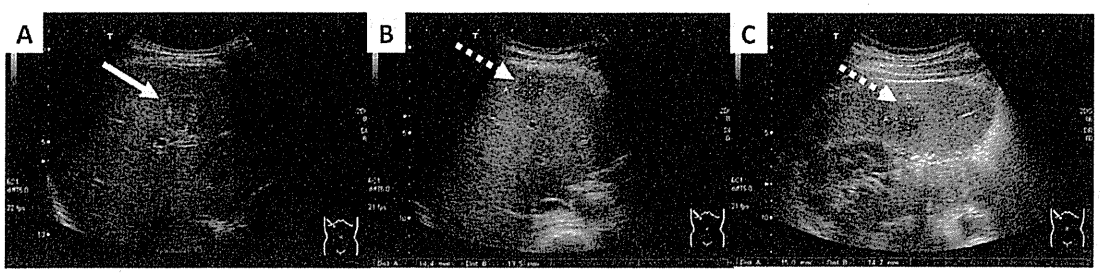

Fig. 1. Ultrasonography showing multiple hypoechoic lesions in the liver. The nodule in segment 5 was diagnosed pathologically as cHCC-CC, which was more sharply-marginated than other nodules, with mosaic pattern internal echo (Panel A, arrow). The other lesions were nonneoplastic (Panel B and C, dotted arrow).

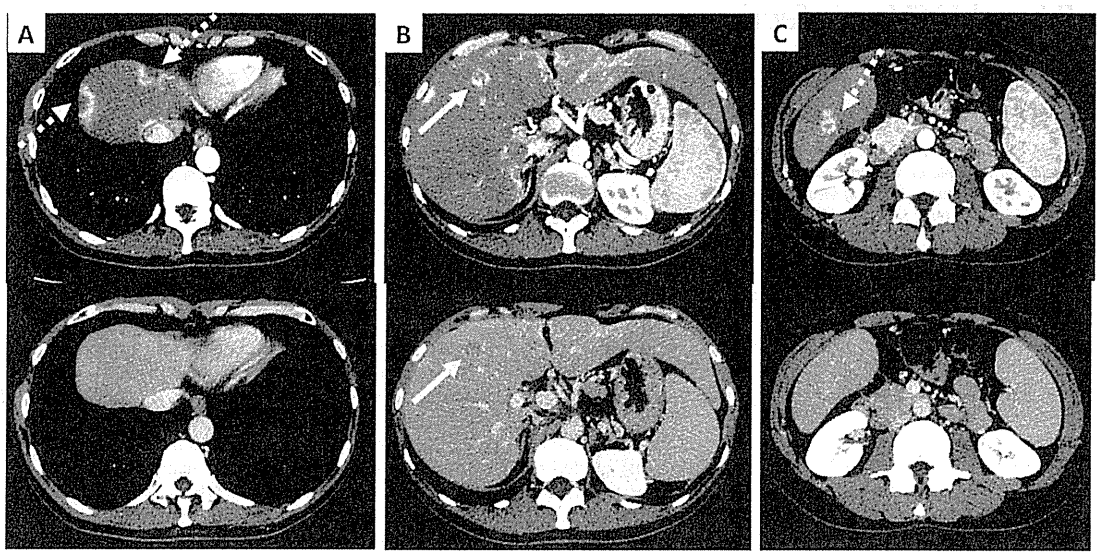

Fig. 2. Contrast-enhanced dynamic CT revealing hyperattenuation in the arterial phase and hypoattenuation in the equilibrium phase in the nodule that was finally diagnosed as cHCC-CC (Panel B, arrow). Other nonneoplastic lesions showed ring-enhancement in the arterial phase without hypoattenuation in the equilibrium phase (Panels A and C, dotted arrow). In each panel, upper image is arterial phase, and lower image is equilibrium phase.

lesions, and the internal echo showed a mosaic pattern (Fig. 1A). Contrast-enhanced dynamic computed tomography (CT) revealed hyperattenuation in the arterial phase and hypoattenuation in the equilibrium phase in the former nodule, suggesting HCC (Fig. 2B). Other lesions showed ring enhancement in the arterial phase without hypoattenuation in the equilibrium phase. Ten or more such lesions were detected. Some of them, which were located near the surface of the liver, presented geographical configuration

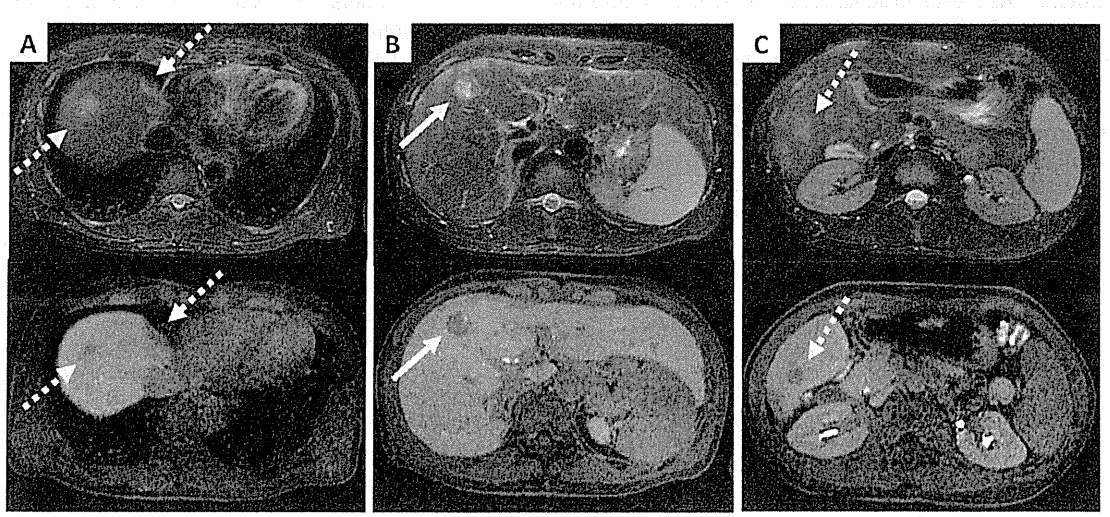

Fig. 3. Gd-EOB-DTPA-enhanced MRI revealing distinct defect in hepatobiliary phase in the nodule of cHCC-CC (down image in Panel B, arrow) and indistinct defect in nonneoplastic lesions (down images in Panels A and C, dotted arrow). In T2-weighted pre-enhancement images, the former nodule showed distinct high intensity (upper image in Panel B, arrow) and the latter showed indistinct slightly high intensity (upper images in Panels A and C, dotted arrow).

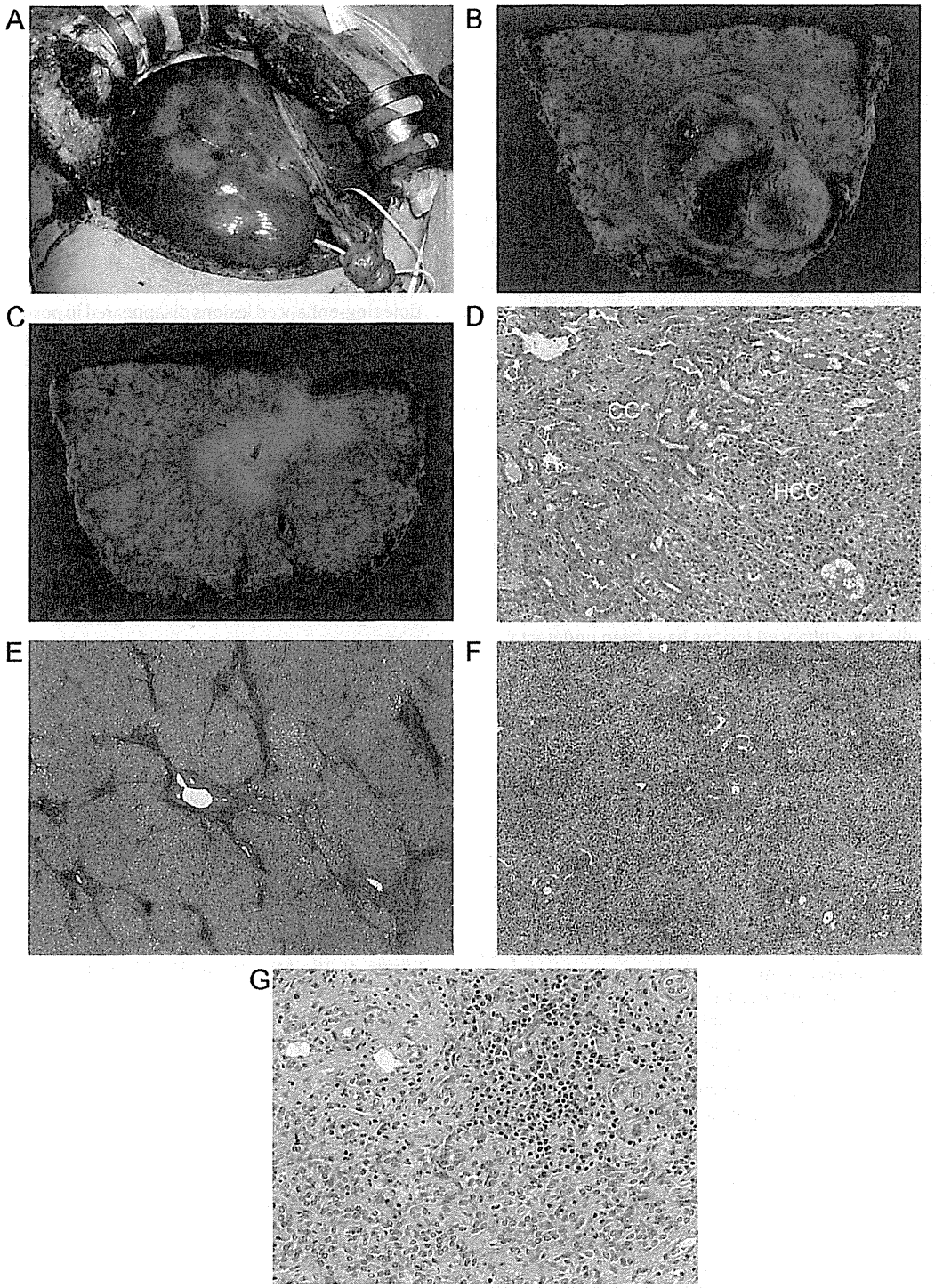

Fig. 4. During the surgery, several white pitted scars were observed on the surface of the liver (Panel A). Gross photograph of resected specimen showed a yellowish-white tumour with capsule (Panel B). Milky white lesions existed in the specimen separated from the tumour (Panel C). The photomicrograph of the cHCC-CC nodule showed both increased cell density with trabecular pattern and pseudoglandular pattern (Panel D, HCC: hepatocellular carcinoma) and irregular glandular structure (Panel D, CC: cholangiocarcinoma). Nonneoplastic lesions showed loss of hepatocytes, lymphoplasmacytic infiltration, proliferation of bile ductules, and mild fibrosis (Panel F and G). The background liver showed chronic hepatitis, F3/A1 in METAVIR system (E).

accompanied by depression, whereas others in inward liver were nodular (Fig. 2A and C). Gadolinium-ethoxybenzyl-diethylenetriamine pentaacetic acid (Gd-EOB-DTPA)-enhanced magnetic resonance imaging (MRI) revealed a distinct defect in the hepatobiliary phase in the nodule suspected of being HCC and an indistinct defect in others (Fig. 3). The enhancement pattern in the arterial phase of each lesion was similar to that in contrast-enhanced CT. Ultrasonography-guided biopsy was performed from the former nodule in segment 5 (Fig. 1A) and a lesion in segment 6 (Fig. 1C). Histological evaluation indicated the nodule in segment

5 to be cHCC-CC. No neoplastic cell was found in the lesion in segment 6.

We considered hyperbilirubinaemia to be due to drug-induced liver injury and changed the anti-HIV regimen, stopping atazanavir and ritonavir and adding raltegravir. Hyperbilirubinaemia was ameliorated thereafter. The patient underwent partial hepatic resection for cHCC-CC. During the surgery, several white pitted scars were observed on the surface of the liver (Fig. 4A). Diagnosis of cHCC-CC of classical type, the HCC component being immunoreactive for Hepatocyte antigen and the CC component for CK7 and CK19, was confirmed by pathological evaluation of the surgical specimen (Fig. 4B and D). In the specimen, there were several lesions of milky white colour that differed from the main tumour, corresponding to the multiple lesions on ultrasonography and CT (Fig. 4C). Pathologically, these lesions showed regional loss of hepatocytes, lymphoplasmacytic infiltration, proliferation of bile ductules and mild fibrosis (Fig. 4F and G). These lesions were localised panlobular necrosis and considered as a non-neoplastic, inflammatory process. Special stains (Gram, Ziehl–Neelsen, Periodic acid-Schiff (PAS) and Grocott) did not reveal any infectious agents, including bacteria, fungus or protozoa (*Toxoplasma*). Immunohistochemical staining for cytomegalovirus and *in situ* hybridisation for EBER were negative. The background liver showed chronic hepatitis, corresponding to F3/A1 in the METAVIR system[4,5] (Fig. 4E).

The patient is currently alive without recurrence for 2 years and the multiple ring-enhanced lesions have been undetectable in postoperative follow-up CT examinations.

3. Other similar and contrasting cases in the literature

This was a case with cHCC-CC accompanied by multiple hypervascular non-neoplastic lesions developed in a patient with HIV and HCV coinfection. In North America, Europe and Japan, HCV infection is the main risk factor for HCC.[6] Several studies also suggested that HCV infection was one of the risk factors for intrahepatic cholangiocarcinoma.[7,8] cHCC-CC is a rare form of primary liver cancer showing histopathological features of both HCC and cholangiocarcinoma.[9,10] As with the present case, cases of cHCC-CC arising from the liver of patients with HCV infection were previously reported in several studies.[11–14] Furthermore, Shaib et al. reported that HIV was one of the risk factors of intrahepatic cholangiocarcinoma along with HCV.[8] Not only HCV but also HIV infection may have played a role in carcinogenesis in this case. There are no other reports of cHCC-CC development in HIV and HCV coinfected patients. There are also no other reports of multiple non-neoplastic hypervascular lesions in the liver of patients undergoing HIV treatment as this case.

4. Discussion

The present case was coinfected with HIV and HCV. Previous studies demonstrated that HIV infection accelerates HCV-related liver-fibrosis progression, and the lower CD4 count is associated with the higher rate of liver-fibrosis progression.[15–17] It was also reported that HCC develops at a younger age and after a shorter period of HCV infection in HIV and HCV coinfected patients than in HCV-monoinfected patients.[18,19] Considering the fact that the present case developed HCC at a younger age than typical HCV-related HCC patients with CD4 count <200 cells μl^{-1}, HIV infection was likely to have accelerated liver fibrosis and carcinogenesis.

This case was also quite interesting in that cHCC-CC and multiple non-neoplastic lesions with impressive radiological findings coexisted in the liver. If based solely on radiologic findings, differential diagnosis would include HCC, cholangiocarcinoma, metastatic liver cancer, malignant lymphoma, epithelioid haemangioendothelioma, hepatic peliosis, Kaposi's sarcoma and inflammatory pseudotumour. Needle biopsy revealed that solitary cHCC-CC and multiple non-neoplastic lesions coexisted. Pathological investigation after surgery suggested that these non-neoplastic lesions were post-inflammatory changes representing residues of panlobular necrosis. Although we suspected fulminant or subacute viral hepatitis or autoimmune hepatitis as a cause of panlobular necrosis, we could not find clinical information that would confirm such diagnosis. We also suspected drug-induced liver injury caused by HAART as a cause of panlobular necrosis. However, there were no other reports of such lesions in the liver of patients receiving HAART. Multiple ring-enhanced lesions disappeared in postoperative follow-up CT, suggesting that they were reversible changes. It may be possible that the multiple non-neoplastic lesions were pathological changes associated with immune disorder caused by HIV infection, immune reconstruction inflammatory syndrome caused by HAART, antiretroviral drug-induced liver injury or infection which we could not diagnose.

Funding

None.

Competing interests

None.

Ethical approval

Not required.

Disclosure

The authors have nothing to disclose.

Acknowledgements

This work was supported in part by Health Sciences Research Grants of The Ministry of Health, Labour and Welfare of Japan (Research on Hepatitis).

References

1. Koziel MJ, Peters MG. Viral hepatitis in HIV infection. *N Engl J Med* 2007;**356**:1445–54.
2. Koike K, Tsukada K, Yotsuyanagi H, Moriya K, Kikuchi Y, Oka S, et al. Prevalence of coinfection with human immunodeficiency virus and hepatitis C virus in Japan. *Hepatol Res* 2007;**37**:2–5.
3. Joshi D, O'Grady J, Dieterich D, Gazzard B, Agarwal K. Increasing burden of liver disease in patients with HIV infection. *Lancet* 2011;**377**:1198–209.
4. The French METAVIR Cooperative Study Group. Intraobserver and interobserver variations in liver biopsy interpretation in patients with chronic hepatitis C. *Hepatology* 1994;**20**:15–20.
5. Bedossa P, Poynard T, The METAVIR Cooperative Study Group. An algorithm for the grading of activity in chronic hepatitis C. *Hepatology* 1996;**24**:289–93.
6. Forner A, Llovet JM, Bruix J. Hepatocellular carcinoma. *Lancet* 2012;**379**:1245–55.
7. Shaib Y, El-Serag HB. The epidemiology of cholangiocarcinoma. *Semin Liver Dis* 2004;**24**:115–25.
8. Shaib YH, El-Serag HB, Davila JA, Morgan R, McGlynn KA. Risk factors of intrahepatic cholangiocarcinoma in the United States: a case-control study. *Gastroenterology* 2005;**128**:620–6.
9. Allen RA, Lisa JR. Combined liver cell and bile duct carcinoma. *Am J Pathol* 1949;**25**:647–55.
10. Goodman ZD, Ishak KG, Langloss JM, Sesterhenn IA, Rabin L. Combined hepatocellular-cholangiocarcinoma. A histologic and immunohistochemical study. *Cancer* 1985;**55**:124–35.
11. Taguchi J, Nakashima O, Tanaka M, Hisaka T, Takazawa T, Kojiro M. A clinicopathological study on combined hepatocellular and cholangiocarcinoma. *J Gastroenterol Hepatol* 1996;**11**:758–64.

12. Jarnagin WR, Weber S, Tickoo SK, Koea JB, Obiekwe S, Fong Y, et al. Combined hepatocellular and cholangiocarcinoma: demographic, clinical, and prognostic factors. *Cancer* 2002;**94**:2040–6.
13. Yano Y, Yamamoto J, Kosuge T, Sakamoto Y, Yamasaki S, Shimada K, et al. Combined hepatocellular and cholangiocarcinoma: a clinicopathologic study of 26 resected cases. *Jpn J Clin Oncol* 2003;**33**:283–7.
14. Cazals-Hatem D, Rebouissou S, Bioulac-Sage P, Bluteau O, Blanche H, Franco D, et al. Clinical and molecular analysis of combined hepatocellular-cholangiocarcinomas. *J Hepatol* 2004;**41**:292–8.
15. Benhamou Y, Bochet M, Di Martino V, Charlotte F, Azria F, Coutellier A, et al. Liver fibrosis progression in human immunodeficiency virus and hepatitis C virus coinfected patients. *Hepatology* 1999;**30**:1054–8.
16. Mohsen AH, Easterbrook PJ, Taylor C, Portmann B, Kulasegaram R, Murad S, et al. Impact of human immunodeficiency virus (HIV) infection on the progression of liver fibrosis in hepatitis C virus infected patients. *Gut* 2003;**52**:1035–40.
17. Yotsuyanagi H, Kikuchi Y, Tsukada K, Nishida K, Kato M, Sakai H, et al. Chronic hepatitis C in patients co-infected with human immunodeficiency virus in Japan: a retrospective multicenter analysis. *Hepatol Res* 2009;**39**:657–63.
18. Garcia-Samaniego J, Rodriguez M, Berenguer J, Rodriguez-Rosado R, Carbo J, Asensi V, et al. Hepatocellular carcinoma in HIV-infected patients with chronic hepatitis C. *Am J Gastroenterol* 2001;**96**:179–83.
19. Brau N, Fox RK, Xiao P, Marks K, Naqvi Z, Taylor LE, et al. Presentation and outcome of hepatocellular carcinoma in HIV-infected patients: a U.S. -Canadian multicenter study. *J Hepatol* 2007;**47**:527–37.

SCIENTIFIC REPORTS

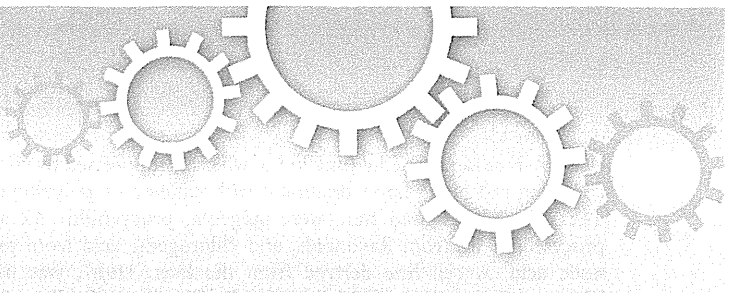

OPEN

SUBJECT AREAS:
MIRNAS
NUTRIENT SIGNALLING
NATURAL PRODUCTS
TYPE 2 DIABETES MELLITUS

Received
10 May 2013

Accepted
15 August 2013

Published
30 August 2013

Correspondence and requests for materials should be addressed to M.O. (otsukamo-tky@umin.ac.jp)

* These authors contributed equally to this work.

The flavonoid apigenin improves glucose tolerance through inhibition of microRNA maturation in miRNA103 transgenic mice

Motoko Ohno[1]*, Chikako Shibata[1]*, Takahiro Kishikawa[1], Takeshi Yoshikawa[1], Akemi Takata[1], Kentaro Kojima[1], Masao Akanuma[2], Young Jun Kang[3], Haruhiko Yoshida[1], Motoyuki Otsuka[1,4] & Kazuhiko Koike[1]

[1]Department of Gastroenterology, Graduate School of Medicine, The University of Tokyo, Tokyo 113-8655, Japan, [2]Division of Gastroenterology, The Institute for Adult Diseases, Asahi Life Foundation, Tokyo 100-0005, Japan, [3]Department of Immunology and Microbial Sciences, The Scripps Research Institute, La Jolla, CA 92037, USA, [4]Japan Science and Technology Agency, PRESTO, Kawaguchi, Saitama 332-0012, Japan.

Polyphenols are representative bioactive substances with diverse biological effects. Here, we show that apigenin, a flavonoid, has suppressive effects on microRNA (miRNA) function. The effects were mediated by impaired maturation of a subset of miRNAs, probably through inhibition of the phosphorylation of TRBP, a component of miRNA-generating complexes via impaired mitogen-activated protein kinase (MAPK) Erk activation. While glucose intolerance was observed in miRNA103 (miR103)-overexpressing transgenic mice, administration of apigenin improved this pathogenic status likely through suppression of matured miR103 expression levels. These results suggest that apigenin may have favorable effects on the pathogenic status induced by overexpression of miRNA103, whose maturation is mediated by phosphorylated TRBP.

Polyphenols, common components of many popular drinks and foods, and caffeine, an alkaloid in various seeds and leaves, are representative bioactive substances with diverse biological effects[1,2]. However, while some effects have been examined in detail[3], the molecular mechanisms underlining these biological effects are mostly undetermined.

MicroRNAs (miRNAs) are short, single-stranded, non-coding RNAs expressed in most organisms ranging from plants to vertebrates[4]. Primary miRNAs, which possess stem-loop structures, are processed into mature miRNAs by Drosha, Dicer, RNA polymerase III, and other related molecules. These mature miRNAs then bind the RNA-induced silencing complex (RISC), and the resulting co-complex directly binds the 3′-untranslated regions (3′-UTRs) of target mRNAs to act as suppressors of translation and gene expression. Thus, dependent upon the identity of the target mRNAs, miRNAs are responsible for the control of various biological functions, including cell proliferation, apoptosis, differentiation, metabolism, oncogenesis, and oncogenic suppression[5–9]. For example, it was reported recently that expression of miRNA103 and 107 (miR103 and 107) was upregulated in obese mice, and that the gain of miR103 function in either liver or fat was sufficient to induce impaired glucose homeostasis[10].

Because the effects of bioactive substances are diverse and the functions of miRNAs result in diverse biological consequences, we hypothesized that some effects of bioactive substances may depend on modulation of miRNA function. In this study, we examined whether polyphenols and caffeine affect miRNA function and determined the molecular mechanisms underlying these effects. In addition, we applied the results obtained here to clinically relevant models to facilitate their use in practical applications.

Results

Apigenin suppresses miRNA function. To determine the effects of polyphenols and caffeine on miRNA function, we determined the luciferase activities of several types of reporters constructed containing

miRNA-binding sites (the function of which is suppressed by corresponding miRNAs) upon treatment with caffeine or polyphenols. The polyphenols used here were apigenin, procyanidin A2 and procyanidin B2 from flavonoids, and chlorogenic acid from phenolic acid. A cell line derived from the liver, Huh7, was used because substances in food theoretically flow into the liver first through the portal vein immediately after intestinal absorption. Among the bioactive substances examined, only apigenin significantly inhibited the effects of miRNAs such as miR122, miR185 and miR103 (Figure 1a), which are highly expressed in the liver[11]. The effects were similarly observed irrespective of endogenous miRNAs or exogenous overexpression of corresponding miRNAs (Figure 1a and b) in a dose-dependent manner (Figure 1c). Another liver cell line, Hep3B, showed similar results, suggesting that the effects were not cell line-specific (Supplementary Figure 1a, b and c). The effects were detected with 5 μM apigenin; this concentration is physiologically attainable[12–14]. These results suggest that apigenin has suppressive effects on miRNA function.

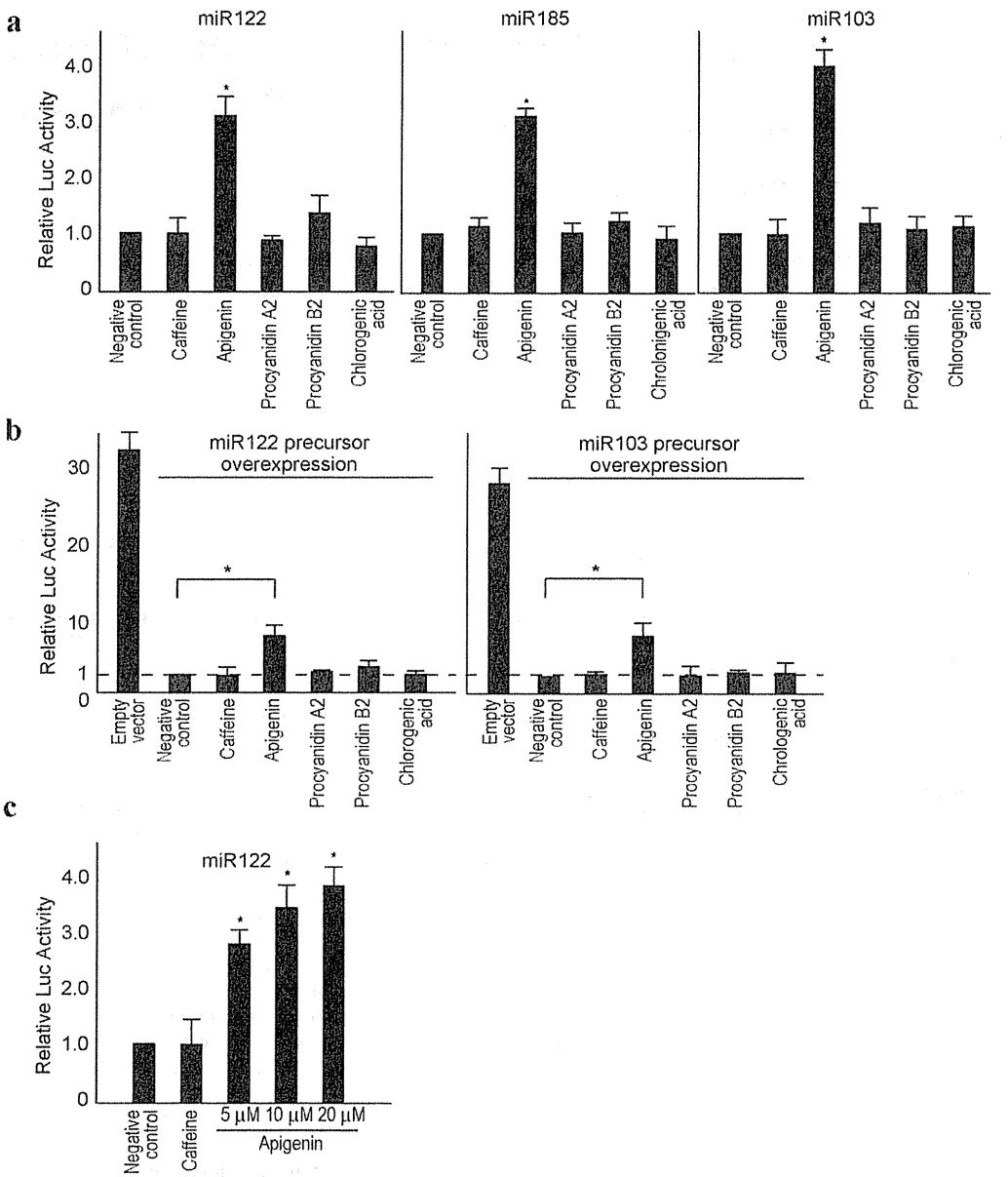

Figure 1 | Apigenin inhibits miRNA function. (a), Apigenin inhibits endogenous miRNA function. Huh7 cells were transfected with reporters to determine the functions of the indicated miRNAs. Twenty-four hours after treatment with the indicated substances, reporter assays were performed. Data represent the means ± standard deviation (s.d.) from three independent experiments. *, $p < 0.05$ (*t*-test). (b), Apigenin inhibits the function of exogenously overexpressed miRNAs. Huh7 cells were transfected with reporters and corresponding miRNA precursor-expressing plasmids or an empty vector. Twenty-four hours after treatment with the indicated substances, reporter assays were performed. Data represent the means ± s.d. from three independent experiments. *, $p < 0.05$ (*t*-test). (c), Dose-dependent effects of apigenin on miRNA function. Huh7 cells were transfected with reporter plasmids to determine miR122 function. Cells were treated with indicated doses of apigenin for 24 h and luciferase assays were performed. Caffeine was included as a negative control. Data represent the means ± s.d. from three independent experiments. *, $p < 0.05$ (*t*-test) compared with the negative control.

Apigenin inhibits miRNA maturation from miRNA precursors. To elucidate the molecular mechanisms underlying the inhibitory effects of apigenin on miRNA function, we first determined the expression levels of miRNA pathway-related molecules including Drosha, DGCR8, KSRP, Argonaute 2 (Ago2), and Dicer in the presence of apigenin. While the expression levels of Drosha, Ago2 and Dicer proteins appeared to decrease slightly after a high dose of apigenin, no significant changes were observed in the expression levels of these proteins (Figure 2a and Supplementary Figure 2a). Next, we examined the expression and maturation of miRNAs by quantitative real-time polymerase chain reaction (qRT-PCR) and Northern blotting (Figure 2b and Supplementary Figure 2b). Expression levels of mature endogenous miR122, miR103, and miR185 decreased and accumulation of precursor miRNAs was also observed after apigenin treatment (Figure 2b), suggesting that maturation from miRNA precursors was decreased. In addition, a comprehensive miRNA microarray analysis confirmed that apigenin altered the expression levels of a major subset of miRNAs (Supplementary Figure 2c; the raw data were deposited in the GEO database; GSE46526). However, some miRNAs, such as let-7, were not affected by apigenin treatment, which was confirmed by qRT-PCR (Figure 2b). These results suggest that apigenin has an inhibitory effect on the maturation of a subset of miRNAs.

Apigenin inhibits phosphorylation of TRBP. The microRNA-generating complex is composed of Dicer and phospho-TRBP isoforms[15], and TRBP phosphorylation enhances the maturation of a subset of miRNAs through stabilization of the microRNA-generating complexes[15]. Phosphorylation of TRBP is mediated by mitogen-activated protein kinase (MAPK) Erk[15]. Because apigenin is known to inhibit Erk activity[16–19], we hypothesized that the inhibitory effects of apigenin on miRNA maturation may be mediated by decreased phosphorylation of TRBP through inhibition of Erk. Consistent with previous reports, although caffeine had no effect on the Erk phosphorylation status, apigenin clearly inhibited Erk phosphorylation 24 h post-treatment without changes in total Erk levels (Figure 3a). Concordantly, SRE-driven reporter activities were diminished by apigenin treatment (Figure 3b), suggesting that apigenin indeed inhibited an Erk-mediated intracellular signaling pathway, consistent with previous reports[16–19]. While TRBP was phosphorylated under normal serum culture conditions, and its phosphorylation status did not change with caffeine treatment, its phosphorylation was inhibited by apigenin (Figure 3c). This effect was confirmed by electrophoresis in a phos-tag gel, which showed a clear slow-migrating band, indicating that TRBP was phosphory lated in control and caffeine-treated conditions, but its phosphorylation was inhibited upon treatment with apigenin (Figure 3d). To confirm that Erk activity was inhibited by apigenin following TRBP phosphorylation, we examined the effects of apigenin using Huh7 cells stably expressing constitutively active Mek1 (CA-MEK) on TRBP phosphorylation. As shown in Figure 3e, the degree of TRBP phosphorylation was increased only by CA-MEK expression, and the augmented phosphorylation was not diminished by apigenin treatment (Figure 3e), suggesting that the effects of apigenin could not be observed under the induced Erk activation. That is, the effects of apigenin were most probably mediated by inhibition of Erk activation. In addition, we established Huh7 cells stably expressing dominant negative Erk (DN-Erk). As predicted, the levels of mature miRNA103, 122, and 185, were decreased in DN-Erk expressing cells, but were slightly increased in CA-MEK expressing cells, irrespective of apigenin treatment (Figure 3f). The expression levels of mature let-7, which were examined as a representative miRNA that was not affected by apigenin treatment in the miRNA microarray (Figure 3f), were not changed by enforced expression of DN-Erk or CA-MEK, suggesting that this miRNA maturation is not significantly regulated by MAPK activity or TRBP phosphorylation, consistent with a previous report[15]. These results suggest that apigenin inhibits Erk phosphorylation, and subsequent decreased MAPK activity leads to a decrease in TRBP phosphorylation, which may result in decreased maturation of a subset of miRNAs.

Apigenin improves glucose tolerance through inhibition of miRNA function. To apply the above results in a clinical setting, we focused on recent findings demonstrating that a gain of miR103/107 expression induces impaired glucose homeostasis *in vivo*[10]. To utilize this, we generated transgenic mice expressing a miR103 precursor under control of the CMV promoter (Supplementary Figure 3a). Overexpression of miR103 in these mice was confirmed by Northern blotting against mature miR103 in liver tissues (Figure 4a and Supplementary Figure 3b). No significant over-saturation of RISC

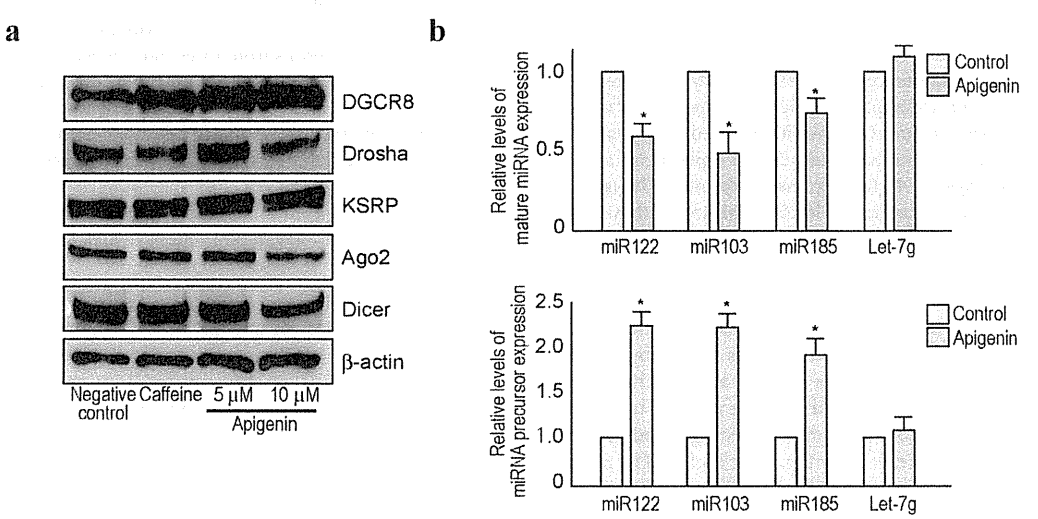

Figure 2 | Apigenin impairs miRNA maturation. (a), Cells were treated with the appropriate substances for 24 h and the indicated proteins were blotted. Representative results from three independent experiments using Huh7 cells are shown. Full-length blot images are available in Supplementary Figure 5a. (b), The expression levels of mature miRNAs and miRNA precursors were determined by qRT-PCR using Huh7 cells with or without apigenin treatment for 24 h. Data represent the means ± s.d. from three independent experiments. *, $p < 0.05$ (t-test) compared with the control (DMSO only) treatment.

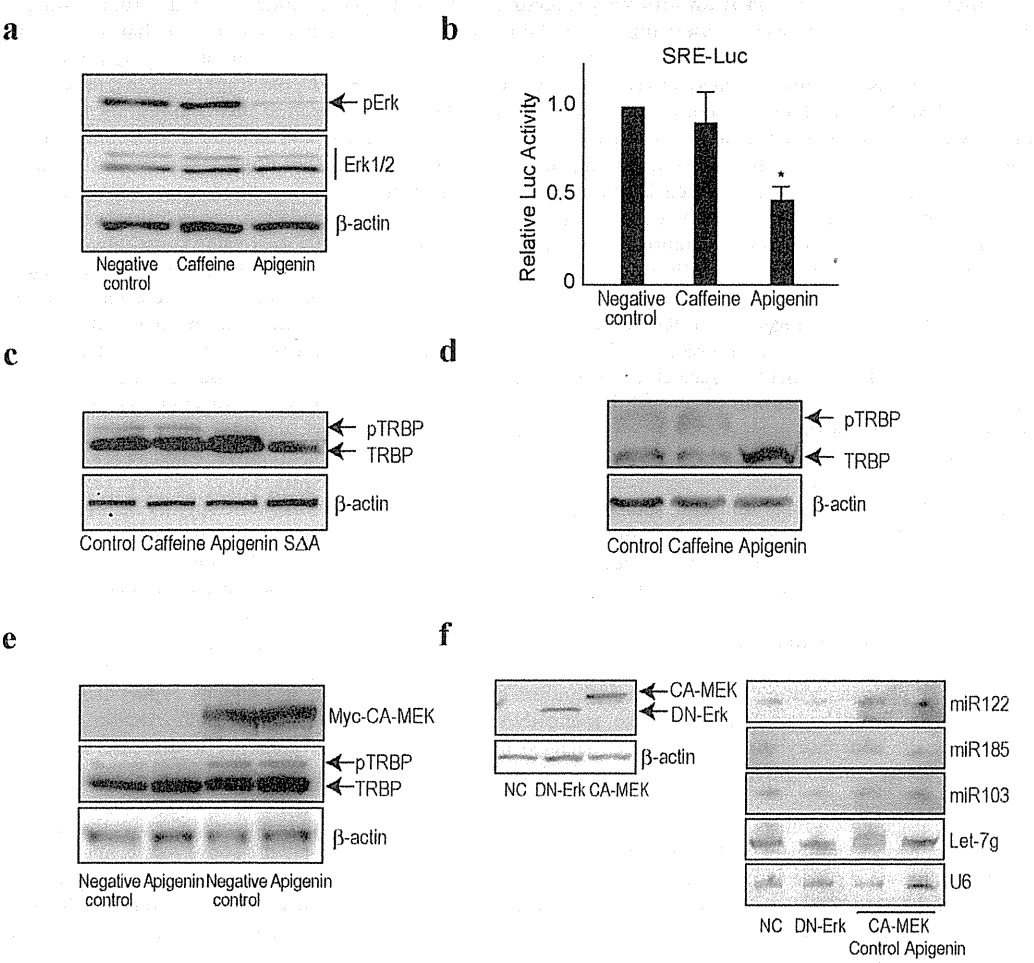

Figure 3 | Apigenin inhibits TRBP phosphorylation. (a), Cells were treated with caffeine or apigenin for 24 h. Cell lysates were blotted with anti-phosphorylated Erk and anti-total Erk1/2. Representative results from three independent experiments using Huh7 cells are shown. Similar results were obtained using Hep3B cells. (b), A luciferase assay was performed to determine SRE-driven transcription under apigenin treatment. Caffeine was included as a comparison. Data represent the means ± s.d. from three independent experiments using Huh7 cells. *, $p < 0.05$ (t-test) compared to the negative control. (c), Huh7 cells were transfected with wild-type TRBP-expressing plasmids followed by treatment with the indicated substances for 24 h. Serine-to-alanine mutant TRBP (SΔA) indicates non-phosphorylated TRBP. Representative results from three independent experiments using Huh7 cells are shown. (d), Substance-treated Huh7 cell lysates were separated using a Mn2+-Phos-tag gel to discriminate the phosphorylated form of TRBP. Representative results from three independent experiments using Huh7 cells are shown. (e), TRBP-expressing Huh7 cells were stably transfected with myc-tagged CA-MEK-expressing plasmids followed by apigenin treatment for 24 h. Phosphorylation status of TRBP was determined by Western blotting. Representative results from three independent experiments are shown. (f), Huh7 cells were stably transfected with myc-tagged CA-MEK-expressing plasmids or myc-tagged DN-Erk-expressing plasmids. The expression of the transfected constructs was confirmed by Western blotting using anti-myc antibodies (left panels). Expression levels of mature miRNAs in those cells with or without apigenin treatment were determined by Northern blotting (right panels). Representative results of at least three independent experiments are shown. Full-length blot images in a, b, c, d, e, and f are available in Supplementary Figure 5b, c, d, e, and f.

complexes due to overexpressing miR103 in these mice was confirmed by a lack of significant changes in the expression levels of other mature miRNAs, such as miR122 and miR185 (Figure 4a). As expected from a previous report[10], these miR103 transgenic mice showed an increase in both random and fasting blood-glucose levels and insulin levels (Supplementary Figure 3c and d). The mean size of adipocytes in visceral fat was larger in normal chow fed miR103 transgenic mice than in control mice, and their size became larger nearly in parallel in both control and miR103 transgenic mice under a high-fat diet (Supplementary Figure 3e).

To determine the effect of apigenin in these models, 40 mg/kg apigenin was intraperitoneally injected daily for 14 days in miR103 transgenic mice. The level of mature miR103 was decreased, and precursors accumulated in apigenin-treated mice, as determined by Northern blotting and qRT-PCR (Figure 4b and Supplementary Figure 4a and b). Similar to the in vitro results, levels of mature miR122 and miR185, but not let-7, in the liver tissues were also decreased by apigenin treatment (Supplementary Figure 4a and b). Phosphorylated TRBP in the liver tissues was decreased in apigenin-treated mice, as determined by a retarded band in the phos-tag gel (Figure 4c), consistent with the *in vitro* results (Figure 3d). Erk phosphorylation was consistently decreased following apigenin treatment (Supplementary Figure 4c). In addition, we confirmed the upregulated expression level of caveolin-1, a major regulator of the insulin receptor, which is a direct target gene of miR103[10] in these tissues (Supplementary Figure 4c). As expected from these results, apigenin-treated miR103 transgenic mice showed decreased random and fasting blood glucose-levels (Figure 4d). While miR103 transgenic mice